Med Chem Res
DOI 10.1007/s00044-016-1562-6

MEDICINAL CHEMISTRY RESEARCH

ORIGINAL RESEARCH

Ferulic acid amide derivatives as anticancer and antioxidant agents: synthesis, thermal, biological and computational studies

Naresh Kumar[1] · Sandeep Kumar[2] · Sheenu Abbat[3] · Kumar Nikhil[1] · Sham M. Sondhi[2] · Prasad V. Bharatam[4] · Partha Roy[1] · Vikas Pruthi[1]

Received: 23 November 2015 / Accepted: 19 March 2016

Abstract The design and microwave-assisted synthesis of four series (**IIIa–IIIo, Va–Vg, VIIa–VIIg** and **IXa–IXe**) of mono and bis-amide derivatives of ferulic acid have been achieved under solvent-free conditions and, subsequently characterized by spectroscopic techniques. During thermal analysis, all the compounds were found stable up to 100 °C and decomposed through single step at higher temperature. The derivatives were screened for their in vitro cytotoxicity and antioxidant activity, respectively and observed that compound **Vb** was most active against breast (MCF-7; IC_{50} = 07.49 μM and MDA-MB-231; IC_{50} = 07.28 μM), **Vd** against lung (A549; IC_{50} = 07.11 μM) and liver (HepG2; IC_{50} = 08.32 μM), and **Ve** against cervical (HeLa; IC_{50} = 07.14 μM) cancer cell lines, while compounds **IIIf, IIIl, IIIo, VIIe** and **IXa–IXe** were found to exhibit the strong antioxidant activity with respect to their parent molecule. Previous reports for the biological applications of ferulic acid amides also confirmed the importance of work presented here. The 3D-QSAR studies for anticancer and antioxidant activities were also performed by using CoMFA, and the corresponding contour maps of electrostatic and steric fields have been computed. Statistical analysis between experimental and CoMFA-predicted data for pIC_{50} have been accomplished by curve fitting analysis which showed the significant correlation.

Graphical Abstract

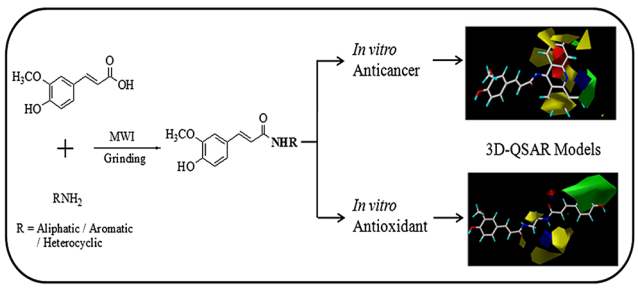

Keywords Ferulic acid · Amide derivatives · Anticancer and antioxidant activity · 3D-QSAR · CoMFA

Introduction

Synthesis of heterocyclic molecules, which can be easily prepared and exhibit good biological activities, is a fascinating area of research (Basoglu *et al.,* 2013). As the limitations of most of the existing anticancer drugs due to various reasons such as drug resistance, serious side effects, and lack of efficiency made infectious diseases a vicious cycle, so there is an urgent need to design improved lead molecules for the well-being of mankind (Narang *et al.,* 2009). The dietary antioxidants are considered to play the shielding role

Electronic supplementary material The online version of this article (doi:10.1007/s00044-016-1562-6) contains supplementary material, which is available to authorized users.

✉ Naresh Kumar
nareshkumariitr@gmail.com

[1] Department of Biotechnology, Indian Institute of Technology Roorkee, Roorkee, Uttarakhand 247667, India

[2] Department of Chemistry, Indian Institute of Technology Roorkee, Roorkee 247667, India

[3] Department of Pharmacoinformatics, NIPER, S.A.S. Nagar, Mohali 160062, India

[4] Department of Medicinal Chemistry, NIPER, S.A.S. Nagar, Mohali 160062, India

Published online: 29 March 2016

against the development and progressions in the pathological conditions produced by oxidative stress, and are involved in many rigorous human diseases mainly including atherosclerosis, cancer, neurodegenerative disorders, diabetes, ageing and many more. Since the last two decades, polyphenols have drawn the attention of scientific community toward their potential antioxidant and other biological effects (Herrmann, 1989; Clifford, 1990; Sajjadi *et al.,* 2004; Wiegand *et al.,* 2009; Ferhat *et al.,* 2014). Ferulic acid is a ubiquitous phenolic derivative of cinnamic acid, exhibits a wide range of biomedical activities viz., anticancer, antioxidant, antimicrobial, anti-inflammatory, antiallergic, antithrombotic, antiviral, hepatoprotective, increases the sperm viability, enhances the stability of cytochrome C and inhibition of apoptosis induced by cytochrome C and increases the IgE binding to peanut allergens, a β-secretase modulator with therapeutic potential against Alzheimer's disease (Rosazza *et al.,* 1995; Mori *et al.,* 1999; Middleton *et al.,* 2000; Toshihiro *et al.,* 2000; Ou and Kwok, 2004; Chung and Champagne, 2011; Mori *et al.,* 2013; Kumar and Pruthi, 2014). In the past few years, different types of ferulic acid derivatives have been discovered which exhibit enhanced biomedical activities as compared to ferulic acid (Hosoda *et al.,* 2002; Tan and Shahidi, 2011; Teresa *et al.,* 2011; Li *et al.,* 2012a, b; Piazzon *et al.,* 2012; Sultana, 2012; Huang *et al.,* 2013; Paiva *et al.,* 2013; Wang *et al.,* 2013; Kiran *et al.,* 2015). The compounds containing amide moiety are also associated with the broad spectrum of biomedical activities (Tamm *et al.,* 2003; Parkesh *et al.,* 2012). Motivated by the wide range of applications shown by ferulic acid alone, different kinds of ferulic acid derivatives and the compounds containing the amide moieties, we had developed a strategy toward the synthesis of different range of novel amide derivatives of ferulic acid by its structural modifications comprising the variety of aliphatic, aromatic and heterocyclic primary amines. Ferulic acid (used in this study) has been extracted and well characterized by single crystal X-ray diffraction along with *p*-coumaric and caffeic acids by our research group (Kumar and Pruthi, 2015; Kumar *et al.,* 2015). The work presented here might serve to provide a new therapeutic approach in the field of medicinal and pharmaceutical chemistry based on the natural sources. The work will also be useful for the design and synthesis of solvent-free molecules which leads to a vital drug.

Materials and methods

Materials

All the reagents used in cell culture were taken from GIBCO (Invitrogen, USA). Penicillin, streptomycin, MTT (3-(4,5-dimethyl-2-thiazolyl)-2,5diphenyl-2H tetrazolium bromide), cell culture grade DMSO, different types of mono- and bis- amines used in synthesis, 5-fluorouracil (5-FU), cyclophosphamide and actidione (cycloheximide) were from HiMedia (Mumbai, India).

Instrumentation

Microwave reactor Anton Paar (monowave 300) and microwave oven model M197DL (Samsung) were used for microwave irradiation. The melting point of compounds were determined by using a JSGW apparatus and are uncorrected. The FT-IR spectra were taken on a PerkinElmer 1600 series FT-IR spectrometer in KBr pellets. All the NMR experiments (^{1}H and ^{13}C-NMR) were carried out on a 500 MHz high-resolution NMR spectrometer (Avance 500 Bruker Biospin Intl. AG, Switzerland) in DMSO-d_6 with tetramethylsilane (TMS) as internal standard. PerkinElmer Clarus 500 gas chromatograph with MS detector built within was used to record the GC–MS, while APCI mass was recorded using Finnigan Mat LCQ mass spectrometer. The elemental analysis has been carried out on a Vario EL III Elementar. Thermogravimetry (TG) and derivative thermogravimetry (DTG) analysis have been carried out by using a mass of 0.045 g at 10 °C/min under the nitrogen at 200 ml/min flow rate on a thermogravimetric analyzer (PerkinElmer's, California, USA). Absorbance of the lysates during MTT assay was determined on a Fluostar optima microplate reader (BMG Labtech, Germany).

General procedure for synthesis of mono and bis amide derivatives of ferulic acid

(E)-3-(4-hydroxy-3-methoxyphenyl)acrylic acid (ferulic acid) and corresponding amines (**IIa–IIo**, **IVa–IVg, VIa–VIg** and **VIIIa–VIIIe**) were mixed together thoroughly in an equimolar ratio for mono-amide and 2:1 molar ratio for bis-amide within a Petri dish. The reaction mixture was subjected to microwave irradiation at 180–450 Watt for 3–7 min. The progress of the reactions was monitored by thin layer chromatography (TLC) on silica gel using ethyl acetate/methanol (4:1, 3:2 and 7:3) as solvent of elution. TLCs indicated the absence of starting materials and confirmed the completion of reaction and formation of products. The crude products thus so obtained were purified by crystallization and re-crystallization in methanol to give the pure products (**IIIa–IIIo, Va–Vg, VIIa–VIIg** and **IXa–IXe**) in high yield.

*(E)-N-cyclopropyl-3-(4-hydroxy-3-methoxyphenyl)acrylamide (**IIIa**)*

Yield: 87 %. Amorphous, bright-yellow. mp: 110–112 °C. FT-IR (KBr, cm^{-1}) ν_{max}: 3435, 2929, 1666, 1606, 1597, 1571. ^{1}H-NMR (500 MHz, DMSO-d_6, *ppm*) δ: 0.37–0.41

(m, 2H, CH_2), 0.56.0.58 (d, 2H, $J = 7$ Hz, CH_2), 2.22–2.24 (m, 1H, CH), 3.81 (s, 3H, OCH_3), 5.44 (s, 1H, NH), 6.34–6.37 (d, 1H, $J = 16$ Hz, Ar), 6.77–6.79 (d, 1H, $J = 8$ Hz, Ar), 7.05–7.07 (d, 1H, $J = 8$ Hz, Ar), 7.26 (s, 1H, Ar), 7.43–7.46 (d, 1H, $J = 16$ Hz, Ar), 10.27 (s, 1H, OH). ^{13}C-NMR (125 MHz, DMSO-*d_6, ppm*) δ: 13.55, 24.10, 56.09, 112.27, 116.44, 117.28, 120.94, 128.77, 144.61, 145.44, 151.17, 166.09. Anal. Calcd. (%) for $C_{13}H_{15}NO_3$ (233.26): C, 66.94; H, 6.48; N, 6.00; Found: C, 66.13; H, 6.29; N, 5.57.

*(E)-N-cyclohexyl-3-(4-hydroxy-3-methoxyphenyl)acrylamide (**IIIb**)*

Yield: 98 %. Crystalline, light-orange. mp: 180–182 °C. FT-IR (KBr, cm^{-1}) ν_{max}: 3435, 2934, 2857, 1689, 1634, 1594. ^{1}H-NMR (500 MHz, DMSO-*d_6, ppm*) δ: 1.13–1.19 (q, 1H, $J = 30$ Hz, $J = 13$ Hz, CH_2), 1.21–1.26 (t, 4H, $J = 25$ Hz, $J = 13$ Hz, $2 \times CH_2$), 1.54–1.57 (d, 1H, $J = 8$ Hz, CH_2), 1.67–1.69 (d, 2H, $J = 12.5$ Hz, CH_2), 1.83–1.85 (d, 2H, $J = 11$ Hz, CH_2), 2.76–2.81 (m, 1H, CH), 3.79 (s, 3H, OCH_3), 5.44 (s, 1H, NH), 6.28–6.32 (d, 1H, $J = 15.5$ Hz, Ar), 6.76–6.77 (d, 1H, $J = 8$ Hz, Ar), 6.96–6.98 (d, 1H, $J = 8.5$ Hz, Ar), 7.16 (s, 1H, Ar), 7.238–7.27 (d, 1H, $J = 16$ Hz, Ar), 10.22 (s, 1H, OH). ^{13}C-NMR (125 MHz, DMSO-*d_6, ppm*) δ: 21.01, 28.54, 33.39, 46.78, 57.32, 112.07, 116.27, 117.58, 120.30, 128.41, 144.33, 145.78, 151.12, 166.67. Anal. Calcd. (%) for $C_{16}H_{21}NO_3$ (275.34): C, 69.79; H, 7.69; N, 5.09; Found: C, 67.63; H, 7.56; N, 4.89.

*(E)-3-(4-hydroxy-3-methoxyphenyl)-N-(2-(pyrrolidin-1-yl)ethyl)acrylamide (**IIIc**)*

Yield: 83 %. Semi-solid, dark-brown. mp: 98–100 °C. FT-IR (KBr, cm^{-1}) ν_{max}: 3407, 2961, 1638, 1597, 1578, 1557. ^{1}H-NMR (500 MHz, DMSO-*d_6, ppm*) δ: 1.67 (s, 4H, $2 \times CH_2$), 2.36–2.54 (m, 6H, $3 \times CH_2$), 2.75–2.78 (t, 2H, $J = 12.5$ Hz, $J = 6.5$ Hz, CH_2), 3.79 (s, 3H, OCH_3), 5.46 (s, 1H, NH), 6.31–6.33 (d, 1H, $J = 15.5$ Hz, Ar), 6.76–6.78 (d, 1H, $J = 8$ Hz, Ar), 6.97–6.99 (d, 1H, $J = 8$ Hz, Ar), 7.17 (s, 1H, Ar), 7.27–7.31 (d, 1H, $J = 15.5$ Hz, Ar), 10.23 (s, 1H, OH). ^{13}C-NMR (125 MHz, DMSO-*d_6, ppm*) δ: 27.10, 37.92, 50.01, 59.01, 112.17, 116.02, 117.18, 120.11, 121.94, 128.23, 129.11, 136.66, 144.21, 145.45, 151.21, 166.36. Anal. Calcd. (%) for $C_{16}H_{22}N_2O_3$ (290.36): C, 66.18; H, 7.64; N, 9.65; Found: C, 65.49; H, 7.54; N, 9.17.

*(E)-3-(4-hydroxy-3-methoxyphenyl)-N-(2-(piperidin-1-yl)ethyl)acrylamide (**IIId**)*

Yield: 87 %. Semi-solid, brown. mp: 98–100 °C. FT-IR (KBr, cm^{-1}) ν_{max}: 3394, 3273, 2935, 2838, 1638, 1593, 1565. ^{1}H-NMR (500 MHz, DMSO-*d_6, ppm*) δ: 1.34 (s, 2H, CH_2), 1.46–1.49 (q, 4H, $J = 5.5$ Hz, $J = 5$ Hz, $2 \times CH_2$), 2.26–2.49 (m, 6H, $3 \times CH_2$), 2.78–2.79 (d, 2H, $J = 5.5$ Hz, CH_2), 3.78 (s, 3H, OCH_3), 5.49 (s, 1H, NH), 6.29–6.33 (d, 1H, $J = 16$ Hz, Ar), 6.76–6.78 (d, 1H, $J = 8$ Hz, Ar), 6.97–6.98 (d, 1H, $J = 6$ Hz, Ar), 7.16 (s, 1H, Ar), 7.27–7.30 (d, 1H, $J = 15.5$ Hz, Ar), 10.23 (s, 1H, OH). ^{13}C-NMR (125 MHz, DMSO-*d_6, ppm*) δ: 25.05, 26.53, 36.99, 53.04, 54.73, 57.09, 112.08, 116.15, 117.16, 120.08, 128.21, 144.15, 145.18, 151.16, 166.80. Anal. Calcd. (%) for $C_{17}H_{24}N_2O_3$ (304.38): C, 67.08; H, 7.95; N, 9.20; Found: C, 66.56; H, 7.89; N, 9.01.

*(E)-3-(4-hydroxy-3-methoxyphenyl)-N-(2,2,6,6-tetramethylpiperidin-4-yl)acrylamide (**IIIe**)*

Yield: 84 %. Crystalline, brick color. mp: 118–120 °C. FT-IR (KBr, cm^{-1}) ν_{max}: 3433, 2961, 1629, 1516. ^{1}H-NMR (500 MHz, DMSO-*d_6, ppm*) δ: 0.98 (s, 2H, CH_2), 1.06 (s, 6H, $2 \times CH_3$), 1.13 (s, 6H, $2 \times CH_3$), 1.71–1.73 (d, 2H, $J = 8.5$ Hz, CH_2), 3.17–3.18 (d, 1H, $J = 7$ Hz, CH), 3.79 (s, 3H, OCH_3), 5.45 (s, 1H, NH), 6.27–6.31 (d, 1H, $J = 16$ Hz, Ar), 6.76–6.77 (d, 1H, $J = 4$ Hz, Ar), 6.95–6.96 (d, 1H, $J = 4$ Hz, Ar), 7.15 (S, 1H, Ar), 7.21–7.24 (d, 1H, $J = 16$ Hz, Ar), 10.24 (s, 1H, OH). ^{13}C-NMR (125 MHz, DMSO-*d_6, ppm*) δ: 29.11, 33.13, 46.01, 47.77, 57.09, 112.12, 116.13, 117.09, 120.17, 128.15, 144.52, 145.66, 151.12, 166.20. Anal. Calcd. (%) for $C_{19}H_{28}N_2O_3$ (332.44): C, 68.65; H, 8.49; N, 8.43; Found: C, 67.82; H, 8.36; N, 8.12.

*(E)-3-(4-hydroxy-3-methoxyphenyl)-N-(3-(2-oxopyrrolidin-1-yl)propyl)acrylamide (**IIIf**)*

Yield: 95 %. Semi-solid, light-brown. mp: 105–107 °C. FT-IR (KBr, cm^{-1}) ν_{max}: 3415, 3150, 2932, 1678, 1609, 1597, 1555. ^{1}H-NMR (500 MHz, DMSO-*d_6, ppm*) δ: 1.53–1.61 (m, 2H, CH_2), 1.87–1.94 (m, 2H, CH_2), 2.19–2.22 (t, 2H, $J = 16$ Hz, $J = 8$ Hz, CH_2), 2.54–2.57 (t, 2H, $J = 14$ Hz, $J = 7$ Hz, CH_2), 3.15–3.19 (t, 2H, $J = 15$ Hz, $J = 8$ Hz, CH_2), 3.21–3.25 (t, 2H, $J = 13$ Hz, $J = 7$ Hz, CH_2), 3.84 (s, 3H, OCH_3), 5.84 (s, 1H, NH), 6.30–6.33 (d, 1H, $J = 16$ Hz, Ar), 6.76–6.77 (d, 1H, $J = 8$ Hz, Ar), 6.99–7.03 (t, 1H, $J = 8$, $J = 7$ Hz, Ar), 7.19–7.19 (d, 1H, $J = 1$ Hz, Ar), 7.29–7.33 (d, 1H, $J = 15.5$ Hz, Ar), 10.27 (s, 1H, OH). ^{13}C-NMR (125 MHz, DMSO-*d_6, ppm*) δ: 17.10, 27.94, 32.10, 37.94, 41.39, 43.03, 56.41, 112.17, 116.36, 117.65, 120.05, 129.34, 144.65, 145.12, 151.15, 166.16, 173.32. Anal. Calcd. (%) for $C_{17}H_{22}N_2O_4$ (318.37): C, 64.13; H, 6.97; N, 8.80; Found: C, 63.74; H, 6.89; N, 8.51.

*(E)-3-(4-hydroxy-3-methoxyphenyl)-N-(2-morpholinoethyl)acrylamide (**IIIg**)*

Yield: 92 %. Crystalline, yellowish-orange. mp: 121–123 °C. FT-IR (KBr, cm^{-1}) ν_{max}: 3431, 3219, 2936, 2820, 1638, 1597. ^{1}H-NMR (500 MHz, DMSO-d_6, *ppm*) δ: 2.35–2.42 (q, 4H, $J = 22$ Hz, $J = 12$ Hz, $2 \times CH_2$), 2.78–2.80 (t, 2H, $J = 12$ Hz, $J = 6$ Hz, CH_2), 3.56–3.57 (t, 6H, $J = 8.5$ Hz, $J = 4.5$ Hz, $3 \times CH_2$), 3.79 (s, 3H, OCH_3), 5.56 (s, 1H, NH), 6.30–6.33 (d, 1H, $J = 15.5$ Hz, Ar), 6.76–6.78 (d, 1H, $J = 8$ Hz, Ar), 6.98–6.99 (d, 1H, $J = 6.5$ Hz, Ar), 7.18 (s, 1H, Ar), 7.29–7.33 (dd, 1H, $J = 7.5$ Hz, $J = 7$ Hz, Ar), 10.28 (s, 1H, OH). ^{13}C-NMR (125 MHz, DMSO-d_6, *ppm*) δ: 37.19, 39.44, 52.04, 54.73, 67.09, 112.21, 116.45, 117.09, 120.88, 128.85, 144.15, 145.68, 151.21, 166.04. Anal. Calcd. (%) for $C_{16}H_{22}N_2O_4$ (306.36): C, 62.73; H, 7.24; N, 9.14; Found: C, 61.84; H, 7.17; N, 8.97.

*(E)-3-(4-hydroxy-3-methoxyphenyl)-N-(2-(piperazin-1-yl)ethyl)acrylamide (**IIIh**)*

Yield: 86 %. Semi-solid, yellowish-brown. mp: 170–172 °C. FT-IR (KBr, cm^{-1}) ν_{max}: 3401, 2995, 2826, 1632, 1585, 1507. ^{1}H-NMR (500 MHz, DMSO-d_6, *ppm*) δ: 2.31–2.34 (d, 6H, $J = 15.5$ Hz, $3 \times CH_2$), 2.71 (s, 6H, $3 \times CH_2$), 3.78–3.79 (d, 3H, $J = 5.5$ Hz, OCH_3), 5.42 (s, 1H, NH), 6.28–6.31 (d, 1H, $J = 16$ Hz, Ar), 6.74–6.77 (t, 1H, $J = 15.5$ Hz, $J = 7.5$ Hz, Ar), 6.96–7.04 (d, 1H, $J = 8.5$ Hz, Ar), 7.17 (s, 1H, Ar), 7.26–7.29 (d, 2H, $J = 15.5$ Hz, Ar), 10.24 (s, 1H, OH). ^{13}C-NMR (125 MHz, DMSO-d_6, *ppm*) δ: 37.11, 46.04, 52.39, 54.74, 57.09, 112.28, 116.45, 117.05, 120.88, 128.14, 144.15, 145.57, 151.05, 166.74. Anal. Calcd. (%) for $C_{16}H_{23}N_3O_3$ (305.37): C, 62.93; H, 7.59; N, 13.76; Found: C, 61.97; H, 7.52; N, 13.31.

*(E)-3-(4-hydroxy-3-methoxyphenyl)-N-(thiophen-2-ylmethyl)acrylamide (**IIIi**)*

Yield: 90 %. Amorphous, coffee color. mp: 111–113 °C. FT-IR (KBr, cm^{-1}) ν_{max}: 3434, 2926, 1685, 1616, 1591, 1564. ^{1}H-NMR (500 MHz, DMSO-d_6, *ppm*) δ: 2.93 (s, 2H, CH_2), 3.81 (s, 3H, OCH_3), 5.46 (s, 3H, NH), 6.33–6.36 (d, 1H, $J = 15.5$ Hz, Ar), 6.77–6.78 (d, 1H, $J = 8$ Hz, Ar), 6.88–6.89 (d, 1H, $J = 2$ Hz, Ar), 6.94–6.96 (q, 1H, $J = 9.5$ Hz, $J = 5.5$ Hz, Ar), 7.02–7.04 (q, 1H, $J = 10.5$ Hz, $J = 8.5$ Hz, Ar), 7.22–7.23 (d, 1H, $J = 2$ Hz, Ar), 7.32–7.34 (d, 1H, $J = 4.5$ Hz, Ar), 7.37–7.39 (d, 1H, $J = 10.5$ Hz, Ar), 10.25 (s, 1H, OH). ^{13}C-NMR (125 MHz, DMSO-d_6, *ppm*) δ: 39.44, 50.41, 56.09, 112.94, 116.12, 117.17, 120.44, 121.61, 128.77, 129.17, 136.11, 144.27, 145.44, 151.28, 166.42. Anal. Calcd. (%) for $C_{15}H_{15}NSO_3$ (289.35): C, 62.26; H, 5.23; N, 4.84; S, 11.08; Found: C, 61.87; H, 5.12; N, 4.59; S, 10.63.

*(E)-3-(4-hydroxy-3-methoxyphenyl)-N-(2-(thiophen-2-yl)ethyl)acrylamide (**IIIj**)*

Yield: 95 %. Amorphous, traditional-brown. mp: 140–142 °C. FT-IR (KBr, cm^{-1}) ν_{max}: 3431, 2930, 2838, 1634, 1593, 1568. ^{1}H-NMR (500 MHz, DMSO-d_6, *ppm*) δ: 2.85–2.87 (t, 2H, $J = 13$ Hz, $J = 6.5$ Hz, CH_2), 2.91–2.95 (q, 2H, $J = 12.5$ Hz, $J = 6.5$ Hz, CH_2), 3.80 (s, 3H, OCH_3), 5.50 (s, 1H, NH), 6.33–6.36 (d, 1H, $J = 15.5$ Hz, Ar), 6.77–6.78 (d, 1H, $J = 8$ Hz, Ar), 6.88–6.89 (d, 1H, $J = 3$ Hz, Ar), 6.94–6.96 (m, 1H, Ar), 7.02–7.04 (dd, 1H, $J = 8$ Hz, $J = 1.5$ Hz, Ar), 7.22–7.23 (s, 1H, Ar), 7.33–7.34 (d, 1H, $J = 4.5$ Hz, Ar), 7.389–7.41 (d, 1H, $J = 15.5$ Hz, Ar), 10.24 (s, 1H, OH). ^{13}C-NMR (125 MHz, DMSO-d_6, *ppm*) δ: 28.39, 38.22, 39.44, 50.41, 112.17, 116.05, 117.17, 120.55, 121.94, 128.21, 129.11, 136.36, 144.21, 145.45, 151.15, 166.51. Anal. Calcd. (%) for $C_{16}H_{17}NSO_3$ (303.38): C, 63.34; H, 5.65; N, 4.62; S, 10.57; Found: C, 62.97; H, 5.53; N, 4.29; S, 10.17.

*(E)-N-(3-(1H-imidazol-1-yl)propyl)-3-(4-hydroxy-3-methoxyphenyl)acrylamide (**IIIk**)*

Yield: 86 %. Crystalline, yellowish-orange. mp: 148–150 °C. FT-IR (KBr, cm^{-1}) ν_{max}: 3413, 3254, 2930, 1636, 1590. ^{1}H-NMR (500 MHz, DMSO-d_6, *ppm*) δ: 1.86–1.89 (q, 2H, $J = 6.5$ Hz, $J = 6$ Hz, CH_2), 2.57–2.59 (t, 2H, $J = 13$ Hz, $J = 6.5$ Hz, CH_2), 3.79 (s, 3H, OCH_3), 4.03–4.05 (q, 2H, $J = 5$ Hz, $J = 4.5$ Hz, CH_2), 5.53 (s, 1H, NH), 6.30–6.34 (d, 1H, $J = 17.5$ Hz, Ar), 6.76–6.78 (d, 1H, $J = 8$ Hz, Ar), 6.88 (s, 1H, Ar), 6.98–7.02 (t, 1H, $J = 19$ Hz, $J = 5.5$ Hz, Ar), 7.17 (s, 2H, Ar), 7.28–7.34 (t, 1H, $J = 30$ Hz, $J = 14.5$ Hz, Ar), 7.63 (s, 1H, Ar), 10.23 (s, 1H, OH). ^{13}C-NMR (125 MHz, DMSO-d_6, *ppm*) δ: 31.03, 38.01, 50.29, 56.57, 112.78, 116.08, 117.08, 120.20, 121.89, 128.01, 128.99, 136.14, 144.21, 145.94, 151.17, 166.15. Anal. Calcd. (%) for $C_{16}H_{19}N_3O_3$ (301.34): C, 63.77; H, 6.36; N, 13.94; Found: C, 62.48; H, 6.24; N, 13.72.

*(E)-N-benzyl-3-(4-hydroxy-3-methoxyphenyl)acrylamide (**IIIl**)*

Yield: 81 %. Crystalline, yellow. mp: 135–137 °C. FT-IR (KBr, cm^{-1}) ν_{max}: 3431, 3007, 2933, 1634, 1598, 1504. ^{1}H-NMR (500 MHz, DMSO-d_6, *ppm*) δ: 3.79 (s, 2H, CH_2), 3.88 (s, 3H, OCH_3), 5.56 (s, 1H, NH), 6.32–6.35 (d, 1H, $J = 15.5$ Hz, Ar), 6.77–6.79 (d, 1H, $J = 8$ Hz, Ar), 7.01–7.03 (d, 1H, $J = 8$ Hz, Ar), 7.21–7.25 (t, 2H, $J = 17.5$ Hz, $J = 10.5$ Hz, Ar), 7.31–7.39 (m, 5H, Ar), 10.27 (s, 1H, OH). ^{13}C-NMR (125 MHz, DMSO-d_6, *ppm*) δ: 45.33, 55.16, 112.14, 116.41, 118.77, 120.14, 126.24, 127.44, 128.17, 129.45, 141.36, 143.58, 145.56, 151.11, 167.24. Anal. Calcd. (%) for $C_{17}H_{17}NO_3$ (283.32): C, 72.07, H, 6.05, N, 4.94; Found: C, 71.26; H, 5.94; N, 4.08.

*(E)-3-(4-hydroxy-3-methoxyphenyl)-N-(pyridin-2-ylmethyl)acrylamide (**IIIm**)*

Yield: 98 %. Semi-solid, brown. mp: 120–122 °C. FT-IR (KBr, cm^{-1}) ν_{max}: 3425, 2895, 1635, 1594, 1557, 1479. ^{1}H-NMR (500 MHz, DMSO-*d_6, ppm*) δ: 3.79 (s, 2H, CH_2), 3.89 (s, 3H, OCH_3), 5.26 (s, 1H, NH), 6.33–6.36 (d, 1H, $J = 16$ Hz, Ar), 6.77–6.79 (d, 1H, $J = 8.5$ Hz, Ar), 7.01–7.02 (d, 1H, $J = 9$ Hz, Ar), 7.03 (s, 1H, Ar), 7.24–7.27 (t, 1H, $J = 8.5$ Hz, $J = 6.5$ Hz, Ar), 7.34–7.38 (d, 1H, $J = 14$ Hz, Ar), 7.44–7.45 (d, 1H, $J = 8$ Hz, Ar), 7.75–7.78 (t, 1H, $J = 15$ Hz, $J = 7.5$ Hz, Ar), 8.50–8.51 (d, 1H, $J = 4$ Hz, Ar), 10.25 (s, 1H, OH). ^{13}C-NMR (125 MHz, DMSO-*d_6, ppm*) δ: 48.21, 55.60, 112.78, 116.33, 118.18, 120.03, 121.21, 124.12, 128.28, 137.12, 144.33, 145.13, 147.14, 151.57, 156.15, 167.37. Anal. Calcd. (%) for $C_{16}H_{16}N_2O_3$ (285.32): C, 67.59; H, 5.67; N, 9.85; Found: C, 66.11; H, 5.63; N, 9.18.

*(E)-3-(4-hydroxy-3-methoxyphenyl)-N-(pyridin-3-ylmethyl)acrylamide (**IIIn**)*

Yield: 96 %. Semi-solid, red–orange. mp: 128–130 °C. FT-IR (KBr, cm^{-1}) ν_{max}: 3425, 2907, 1636, 1586, 1511. ^{1}H-NMR (500 MHz, DMSO-*d_6, ppm*) δ: 3.76 (s, 2H, CH_2), 3.80 (s, 3H, OCH_3), 5.24 (s, 1H, NH), 6.33–6.36 (d, 1H, $J = 16$ Hz, Ar), 6.77–6.79 (d, 1H, $J = 8$ Hz, Ar), 7.04–7.05 (d, 1H, $J = 8$ Hz, Ar), 7.242 (s, 1H, Ar), 7.32–7.34 (q, 1H, $J = 12.5$ Hz, $J = 5$ Hz, Ar), 7.40–7.44 (d, 1H, $J = 16$ Hz, Ar), 7.44–7.46 (d, 1H, $J = 7.5$ Hz, Ar), 8.42–8.43 (d, 1H, $J = 4.5$ Hz, Ar), 8.53 (s, 1H, Ar), 10.27 (s, 1H, 1 × OH). ^{13}C-NMR (125 MHz, DMSO-*d_6, ppm*) δ: 45.01, 55.63, 112.16, 116.33, 118.02, 120.03, 121.24, 124.29, 128.17, 137.55, 144.36, 145.13, 147.75, 151.37, 156.28, 167.45. Anal. Calcd. (%) for $C_{16}H_{16}N_2O_3$ (285.32): C, 67.59; H, 5.67; N, 9.85; Found: C, 66.23; H, 5.62; N, 9.12.

*(E)-3-(4-hydroxy-3-methoxyphenyl)-N-(pyridin-4-ylmethyl)acrylamide (**IIIo**)*

Yield: 98 %. Crystalline, yellow. mp: 160–162 °C. FT-IR (KBr, cm^{-1}) ν_{max}: 3431, 3002, 1636, 1595, 1520, 1459. ^{1}H-NMR (500 MHz, DMSO-*d_6, ppm*) δ: 3.77 (s, 2H, CH_2), 3.80 (s, 3H, OCH_3), 5.43 (s, 1H, NH), 6.34–6.37 (d, 1H, $J = 14.5$ Hz, Ar), 6.77–6.78 (d, 1H, $J = 8.5$ Hz, Ar), 7.04–7.06 (d, 1H, $J = 8$ Hz, Ar), 7.25 (s, 1H, Ar), 7.35–7.36 (d, 2H, $J = 4.5$ Hz, Ar), 7.42–7.45 (d, 1H, $J = 14.5$ Hz, Ar), 8.47–8.48 (d, 2H, $J = 5$ Hz, Ar), 10.23 (s, 1H, OH). ^{13}C-NMR (125 MHz, DMSO-*d_6, ppm*) δ: 44.27, 55.32, 112.07, 116.02, 118.58, 120.44, 124.41, 128.78, 144.33, 145.78, 147.81, 149.15, 151.82, 167.18. Anal. Calcd. (%) for $C_{16}H_{16}N_2O_3$ (285.32): C, 67.59; H, 5.67; N, 9.85; Found: C, 66.03; H, 5.59; N, 9.09.

*(E)-N-(acridin-9-yl)-3-(4-hydroxy-3-methoxyphenyl)acrylamide (**Va**)*

Yield: 85 %. Amorphous, aureolin-yellow. mp: 262–264 °C. FT-IR (KBr, cm^{-1}): 3331, 3172, 1649, 1616, 1589, 1558. ^{1}H-NMR (500 MHz, DMSO-*d_6, ppm*) δ: 3.79 (s, 3H, 1 × OCH_3), 5.44 (s, 1H, 1 × NH), 6.28–6.31 (d, 1H, $J = 15.5$ Hz, Ar), 6.75–6.77 (d, 1H, $J = 8$ Hz, Ar), 6.96–6.98 (d, 1H, $J = 8.5$ Hz, Ar), 7.16 (s, 1H, Ar), 7.24–7.27 (d, 1H, $J = 11$ Hz, Ar), 7.38–7.41 (d, 2H, $J = 15$ Hz, $J = 7.5$ Hz, Ar), 7.47–7.49 (d, 2H, $J = 8.5$ Hz, Ar), 7.77–7.80 (q, 2H, $J = 15.5$ Hz, $J = 7.5$ Hz, Ar), 8.07–8.09 (d, 2H, $J = 9$ Hz, Ar), 10.21 (s, 1H, OH). ^{13}C-NMR (125 MHz, DMSO-*d_6, ppm*) δ: 56.14, 112.98, 114.22, 116.17, 118.13, 120.11, 124.22, 126.13, 128.55, 129.11, 129.98, 144.15, 144.99, 148.14, 151.36, 164.55, 167.75. Anal. Calcd. (%) for $C_{23}H_{18}N_2O_3$ (370.40): C, 74.58; H, 4.90; N, 7.56; Found: C, 73.17; H, 4.79; N, 7.09.

*(E)-3-(4-hydroxy-3-methoxyphenyl)-N-(4-methylacridin-9-yl)acrylamide (**Vb**)*

Yield: 88 %. Amorphous, corn-yellow. mp: 271–273 °C. FT-IR (KBr, cm^{-1}): 3378, 3121, 1646, 1618, 1593, 1562. ^{1}H-NMR (500 MHz, DMSO-*d_6, ppm*) δ: 2.28 (s, 3H, CH_3), 3.78 (s, 3H, OCH_3), 5.49 (s, 1H, NH), 6.28–6.31 (d, 1H, $J = 15$ Hz, Ar), 6.75–6.78 (m, 2H, Ar), 6.96–6.98 (d, 1H, $J = 9$ Hz, Ar), 7.16–7.18 (q, 2H, $J = 10.5$ Hz, $J = 4.5$ Hz, Ar), 7.27–7.29 (t, 2H, $J = 13$ Hz, $J = 7.5$ Hz, Ar), 7.38–7.41 (t, 1H, $J = 15$ Hz, $J = 7.5$ Hz, Ar), 7.47–7.49 (d, 1H, $J = 8.5$ Hz, Ar), 7.77–7.79 (d, 1H, $J = 9.5$ Hz, Ar), 8.07–8.09 (d, 1H, $J = 9$ Hz, Ar), 10.24 (s, 1H, OH). ^{13}C-NMR (125 MHz, DMSO-*d_6, ppm*) δ: 22.39, 56.10, 108.55, 112.45, 116.16, 118.38, 119.34, 120.81, 122.22, 126.23, 127.12, 128.22, 128.78, 129.13, 129.97, 130.99, 136.11, 144.14, 145.11, 148.14, 151.36, 155.44, 164.14, 167.15. Anal. Calcd. (%) for $C_{24}H_{20}N_2O_3$ (384.43): C, 74.98; H, 5.24; N, 7.29; Found: C, 74.21; H, 5.13; N, 6.91.

*(E)-3-(4-hydroxy-3-methoxyphenyl)-N-(3-methylacridin-9-yl)acrylamide (**Vc**)*

Yield: 89 %. Amorphous, coyote-brown. mp: 259–261 °C. FT-IR (KBr, cm^{-1}): 3391, 3211 1641, 1607, 1591, 1555. ^{1}H-NMR (500 MHz, DMSO-*d_6, ppm*) δ: 2.27 (s, 3H, CH_3), 3.79 (s, 3H, OCH_3), 5.49 (s, 1H, NH), 6.28–6.31 (d, 1H, $J = 15$ Hz, Ar), 6.76–6.78 (d, 2H, $J = 13$ Hz, Ar), 6.95–6.98 (m, 2H, Ar), 7.16–7.18 (q, 2H, $J = 14.5$ Hz, $J = 9.5$ Hz, Ar), 7.27–7.30 (q, 2H, $J = 15.5$ Hz, $J = 10.5$ Hz, Ar), 7.38–7.41 (t, 1H, $J = 15.5$ Hz, $J = 7.5$ Hz, Ar), 7.47–7.49 (d, 1H, $J = 9.5$ Hz, Ar), 7.78–7.79 (d, 1H, $J = 9$ Hz, Ar), 8.07–8.09 (d, 1H, $J = 10.5$ Hz, Ar), 10.22 (s, 1H, OH). ^{13}C-NMR (125 MHz,

DMSO-d_6, *ppm*) δ: 26.08, 56.01, 107.11, 112.13, 116.11, 118.38, 119.33, 120.82, 122.11, 127.23, 127.79, 128.22, 128.88, 129.12, 129.98, 131.83, 139.44, 144.11, 145.99, 147.44, 148.33, 151.14, 164.31, 167.32. Anal. Calcd. (%) for $C_{24}H_{20}N_2O_3$ (384.43): C, 74.98; H, 5.24; N, 7.29; Found: C, 73.67; H, 5.15; N, 6.69.

*(E)-3-(4-hydroxy-3-methoxyphenyl)-N-(2-methylacridin-9-yl)acrylamide (**Vd**)*

Yield: 88 %. Amorphous, buff-yellow. mp: 262–264 °C. FT-IR (KBr, cm^{-1}): 3331, 3201, 1638, 1603, 1586, 1553. ^{1}H-NMR (500 MHz, DMSO-d_6, *ppm*) δ: 2.27 (s, 3H, CH_3), 3.66 (s, 3H, OCH_3), 5.52 (s, 1H, NH), 6.28–6.32 (d, 1H, $J = 14.5$ Hz, Ar), 6.75–6.78 (d, 1H, $J = 14.5$ Hz, Ar), 6.95–6.98 (m, 2H, Ar), 7.15–7.18 (q, 2H, $J = 15$ Hz, $J = 9.5$ Hz, Ar), 7.27–7.30 (q, 2H, $J = 12.5$ Hz, $J = 7$ Hz, Ar), 7.38–7.41 (t, 1H, $J = 16$ Hz, $J = 7.5$ Hz, Ar), 7.47–7.49 (d, 1H, $J = 10$ Hz, Ar), 7.77–7.79 (d, 1H, $J = 10$ Hz, Ar), 8.07–8.09 (d, 1H, $J = 10.5$ Hz, Ar), 10.09 (s, 1H, OH). ^{13}C-NMR (125 MHz, DMSO-d_6, *ppm*) δ: 27.27, 55.33, 107.24, 112.12, 116.26, 118.39, 119.39, 120.27, 121.03, 127.12, 128.02, 128.32, 128.88, 129.24, 130.84, 133.19, 135.42, 144.19, 145.92, 146.43, 148.33, 151.15, 164.31, 167.51. Anal. Calcd. (%) for $C_{24}H_{20}N_2O_3$ (384.43): C, 74.98; H, 5.24; N, 7.29; Found: C, 73.53; H, 5.13; N, 6.51.

*(E)-3-(4-hydroxy-3-methoxyphenyl)-N-(4-methoxyacridin-9-yl)acrylamide (**Ve**)*

Yield: 91 %. Amorphous, yellowish-green. mp: 281–283 °C. FT-IR (KBr, cm^{-1}): 3403, 3151, 1642, 1609, 1591, 1558. ^{1}H-NMR (500 MHz, DMSO-d_6, *ppm*) δ: 3.78 (s, 3H, OCH_3), 3.88 (s, 3H, OCH_3), 5.46 (s, 1H, NH), 6.28–6.31 (d, 1H, $J = 15$ Hz, Ar), 6.75–6.78 (m, 2H, Ar), 6.96–6.98 (d, 1H, $J = 7.5$ Hz, Ar), 7.16–7.18 (q, 2H, $J = 12.5$ Hz, $J = 6.5$ Hz, Ar), 7.27–7.31 (q, 2H, $J = 18.5$ Hz, $J = 11.5$ Hz, Ar), 7.38–7.41 (t, 1H, $J = 15$ Hz, $J = 8.5$ Hz, Ar), 7.47–7.49 (d, 1H, $J = 10$ Hz, Ar), 7.75–7.78 (d, 1H, $J = 11$ Hz, Ar), 8.08–8.10 (d, 1H, $J = 10$ Hz, Ar), 10.32 (s, 1H, OH). ^{13}C-NMR (125 MHz, DMSO-d_6, *ppm*) δ: 55.21, 56.09, 106.24, 108.10, 112.27, 113.33, 116.34, 118.27, 120.03, 122.13, 125.09, 127.12, 128.08, 128.13, 129.83, 130.14, 139.43, 144.19, 144.92, 148.44, 151.14, 156.15, 164.11, 167.19. Anal. Calcd. (%) for $C_{24}H_{20}N_2O_4$ (400.43): C, 71.99; H, 5.03; N, 7.00; Found: C, 71.16; H, 4.93; N, 6.43.

*(E)-3-(4-hydroxy-3-methoxyphenyl)-N-(3-methoxyacridin-9-yl)acrylamide (**Vf**)*

Yield: 93 %. Amorphous, arctic-lime. mp: 278–280 °C. FT-IR (KBr, cm^{-1}): ^{1}H-NMR (500 MHz, DMSO-d_6, *ppm*) δ: 3.69 (s, 3H, OCH_3), 3.79 (s, 3H, OCH_3), 5.51 (s, 1H, NH), 6.28–6.31 (d, 1H, $J = 14.5$ Hz, Ar), 6.75–6.78 (d, 1H, $J = 15$ Hz, Ar), 6.94–6.98 (m, 2H, Ar), 7.15–7.18 (q, 2H, $J = 15.5$ Hz, $J = 11$ Hz, Ar), 7.27–7.31 (q, 2H, $J = 18.5$ Hz, $J = 10.5$ Hz, Ar), 7.38–7.41 (t, 1H, $J = 15.5$ Hz, $J = 7.5$ Hz, Ar), 7.47–7.49 (d, 1H, $J = 9.5$ Hz, Ar), 7.77–7.79 (d, 1H, $J = 10$ Hz, Ar), 8.07–8.09 (d, 1H, $J = 11$ Hz, Ar), 10.33 (s, 1H, OH). ^{13}C-NMR (125 MHz, DMSO-d_6, *ppm*) δ: 55.73, 56.36, 105.44, 107.29, 112.53, 116.83, 117.29, 118.24, 118.53, 120.16, 122.99, 127.12, 128.08, 128.91, 129.13, 129.82, 144.83, 145.11, 148.92, 150.13, 151.79, 159.52, 164.23, 167.19. Anal. Calcd. (%) for $C_{24}H_{20}N_2O_4$ (400.43): C, 71.99; H, 5.03; N, 7.00; Found: C, 70.33; H, 4.97; N, 6.55.

*(E)-3-(4-hydroxy-3-methoxyphenyl)-N-(2-methoxyacridin-9-yl)acrylamide (**Vg**)*

Yield: 90 %. Amorphous, yellow. mp: 275–277 °C. FT-IR (KBr, cm^{-1}): 3407, 3161, 1642, 1611, 1581, 1567. ^{1}H-NMR (500 MHz, DMSO-d_6, *ppm*) δ: 3.67 (s, 3H, OCH_3), 3.78 (s, 3H, OCH_3), 5.46 (s, 1H, NH), 6.29–6.32 (d, 1H, $J = 15$ Hz, Ar), 6.77–6.81 (d, 1H, $J = 15$ Hz, Ar), 6.94–6.98 (m, 2H, Ar), 7.16–7.19 (q, 2H, $J = 14$ Hz, $J = 9$ Hz, Ar), 7.27–7.30 (q, 2H, $J = 16.5$ Hz, $J = 11.5$ Hz, Ar), 7.38–7.41 (t, 1H, $J = 18$ Hz, $J = 10.5$ Hz, Ar), 7.47–7.49 (d, 1H, $J = 8.5$ Hz, Ar), 7.78–7.79 (d, 1H, $J = 10$ Hz, Ar), 8.07–8.09 (d, 1H, $J = 10$ Hz, Ar), 10.46 (s, 1H, OH). ^{13}C-NMR (125 MHz, DMSO-d_6, *ppm*) δ: 55.51, 56.45, 105.21, 108.11, 112.32, 116.33, 118.31, 120.23, 121.53, 123.86, 127.09, 128.12, 128.77, 129.08, 129.71, 130.13, 143.83, 144.81, 144.92, 147.43, 151.19, 156.52, 163.10, 167.12. Anal. Calcd. (%) for $C_{24}H_{20}N_2O_4$ (400.43): C, 71.99; H, 5.03; N, 7.00; Found: C, 70.21; H, 4.94; N, 6.18.

*Synthesis of (E)-3-(4-hydroxy-3-methoxyphenyl)-N-phenylacrylamide (**VIIa**)*

Yield: 97 %. Crystalline, black-olive. mp: 138–140 °C. FT-IR (KBr, cm^{-1}): 3434, 3292, 1664, 1614, 1513, 1429, 1322, 1274, 1203, 1173, 1108, 1032. ^{1}H-NMR (500 MHz, DMSO-d_6, *ppm*) δ: 3.78 (s, 3H, OCH_3), 6.32–6.35 (d, 1H, $J = 16$ Hz, Ar), 6.77–6.78 (d, 1H, $J = 8$ Hz, Ar), 7.01–7.03 (d, 1H, $J = 8$ Hz, Ar), 7.21–7.25 (t, 2H, $J = 21$ Hz, $J = 21$ Hz, Ar), 7.30–7.34 (m, 5H, Ar), 8.39 (s, 1H, NH), 10.37 (s, 1H, OH). ^{13}C-NMR (125 MHz, DMSO-d_6, *ppm*) δ: 56.32, 112.08, 116.07, 118.44, 120.58, 121.30, 124.41, 128.33, 129.34, 135.78, 144.11, 149.17, 151.45, 166.12. Anal. Calcd. (%) for $C_{16}H_{15}NO_3$ (269.29): C, 71.36, H, 5.61, N, 5.20; Found: C, 70.11, H, 5.57, N, 4.93.

(E)-3-(4-hydroxy-3-methoxyphenyl)-N–o-tolylacrylamide ***(VIIb)***

Yield: 87 %. Amorphous, yellow. mp: 162–164 °C. FT-IR (KBr, cm^{-1}): 3436, 3015, 2968, 1691, 1665, 1619, 1597. ^{1}H-NMR (500 MHz, DMSO-*d_6, ppm*) δ: 2.74 (s, 3H, CH_3), 3.79 (s, 3H, OCH_3), 6.33–6.36 (d, 1H, $J = 19$ Hz, Ar), 6.77–6.79 (d, 1H, $J = 8$ Hz, Ar), 7.01–7.02 (d, 1H, $J = 7.5$ Hz, Ar), 7.21 (s, 1H, Ar), 7.24–7.27 (t, 1H, $J = 13.5$ Hz, $J = 8$ Hz, Ar), 7.34–7.37 (d, 1H, $J = 15.5$ Hz, Ar), 7.43–7.45 (d, 1H, $J = 8$ Hz, Ar), 7.76–7.78 (d, 1H, $J = 9$ Hz, Ar), 8.50–8.51 (d, 1H, $J = 2.5$ Hz, Ar), 8.95 (s, 1H, NH), 10.24 (s, 1H, OH). ^{13}C-NMR (125 MHz, DMSO-*d_6, ppm*) δ: 16.33, 56.09, 112.11, 116.02, 118.04, 120.83, 121.51, 124.49, 126.49, 128.54, 129.33, 134.80, 135.78, 144.14, 145.49, 151.46, 166.05. Anal. Calcd. (%) for $C_{17}H_{17}NO_3$ (283.32): C, 72.07, H, 6.05, N, 4.94; Found: C, 71.43, H, 5.97, N, 4.01.

(E)-3-(4-hydroxy-3-methoxyphenyl)-N-m-tolylacrylamide ***(VIIc)***

Yield: 80 %. Crystalline, brass color. mp: 164–166 °C. FT-IR (KBr, cm^{-1}): 3435, 3189, 3014, 1690, 1665, 1618, 1584, 1564. ^{1}H-NMR (500 MHz, DMSO-*d_6, ppm*) δ: 2.86 (s, 3H, CH_3), 3.84 (s, 3H, OCH_3), 6.32–6.36 (d, 1H, $J = 17$ Hz, Ar), 6.77–6.79 (d, 1H, $J = 7$ Hz, Ar), 7.04–7.06 (d, 1H, $J = 9$ Hz, Ar), 7.24 (s, 1H, Ar), 7.31–7.34 (m, 1H, Ar), 7.41–7.44 (d, 1H, $J = 14$ Hz, Ar), 7.74–7.76 (d, 1H, $J = 8$ Hz, Ar), 8.41–8.42 (d, 1H, $J = 3.5$ Hz, Ar), 8.53 (s, 1H, Ar), 8.87 (s, 1H, NH), 10.24 (s, 1H, OH). ^{13}C-NMR (125 MHz, DMSO-*d_6, ppm*) δ: 26.44, 56.01, 112.11, 116.01, 118.04, 119.21, 120.82, 121.51, 124.49, 128.54, 129.32, 135.80, 138.78, 144.14, 145.49, 151.45, 167.04. Anal. Calcd. (%) for $C_{17}H_{17}NO_3$ (283.32): C, 72.07, H, 6.05, N, 4.94; Found: C, 71.21, H, 5.92, N, 4.17.

(E)-3-(4-hydroxy-3-methoxyphenyl)-N-p-tolylacrylamide ***(VIId)***

Yield: 83 %. Crystalline, gray. mp: 158–160 °C. FT-IR (KBr, cm^{-1}): 3436, 3015, 2978, 1691, 1665, 1619, 1597, 1515, 1464, 1431, 1379, 1273, 1206, 1177, 1113, 1034. ^{1}H-NMR (500 MHz, DMSO-*d_6, ppm*) δ: 2.85 (s, 3H, CH_3), 3.83 (s, 3H, OCH_3), 6.33–6.36 (d, 1H, $J = 14$ Hz, Ar), 6.77–6.79 (d, 1H, $J = 8.5$ Hz, Ar), 7.04–7.06 (d, 1H, $J = 8$ Hz, Ar), 7.25 (s, 1H, Ar), 7.35–7.36 (d, 2H, $J = 4.5$ Hz, Ar), 7.42–7.45 (d, 1H, $J = 15.5$ Hz, Ar), 8.47–8.48 (d, 2H, $J = 5$ Hz, Ar), 8.88 (s, 1H, NH), 10.25 (s, 1H, OH). ^{13}C-NMR (125 MHz, DMSO-*d_6, ppm*) δ: 26.83, 56.51, 112.54, 116.01, 118.14, 120.82, 121.45, 127.55, 129.52, 132.80, 134.97, 144.14, 145.49, 151.45, 167.28. Anal. Calcd. (%) for $C_{17}H_{17}NO_3$ (283.32): C, 72.07, H, 6.05, N, 4.94; Found: C, 71.09, H, 5.94, N, 4.05.

(E)-3-(4-hydroxy-3-methoxyphenyl)-N-(2-methoxyphenyl)acrylamide ***(VIIe)***

Yield: 79 %. Crystalline, brown. mp: 174–176 °C. FT-IR (KBr, cm^{-1}): 3437, 3377, 1691, 1645, 1620, 1588, 1563. ^{1}H-NMR (500 MHz, DMSO-*d_6, ppm*) δ: 3.70 (s, 3H, OCH_3), 3.80 (s, 3H, OCH_3), 6.33–6.37 (d, 1H, $J = 19$ Hz, Ar), 6.77–6.79 (d, 1H, $J = 8$ Hz, Ar), 7.01–7.02 (d, 1H, $J = 8$ Hz, Ar), 7.21 (s, 1H, Ar), 7.24–7.27 (t, 1H, $J = 13$ Hz, $J = 6.5$ Hz, Ar), 7.34–7.37 (d, 1H, $J = 15$ Hz, Ar), 7.43–7.45 (d, 1H, $J = 8$ Hz, Ar), 7.76–7.78 (t, 1H, $J = 13$ Hz, $J = 4$ Hz, Ar), 8.50–8.51 (d, 1H, $J = 3.5$ Hz, Ar), 8.98 (s, 1H, NH), 10.37 (s, 1H, OH). ^{13}C-NMR (125 MHz, DMSO-*d_6, ppm*) δ: 56.01, 56.99, 112.11, 116.01, 118.05, 120.83, 121.34, 124.77, 126.49, 128.57, 129.33, 134.80, 135.78, 144.14, 145.49, 151.42, 167.01. Anal. Calcd. (%) for $C_{17}H_{17}NO_4$ (299.32): C, 68.22, H, 5.72, N, 4.68; Found: C, 67.37, H, 5.67, N, 4.02.

(E)-3-(4-hydroxy-3-methoxyphenyl)-N-(3-methoxyphenyl)acrylamide ***(VIIf)***

Yield: 84 %. Crystalline, gray. mp: 128–130 °C. FT-IR (KBr, cm^{-1}): 3433, 3347, 1689, 1663, 1623, 1596, 1560. ^{1}H-NMR (500 MHz, DMSO-*d_6, ppm*) δ: 3.71 (s, 3H, OCH_3), 3.80 (s, 3H, OCH_3), 6.33–6.36 (d, 1H, $J = 17$ Hz, Ar), 6.77–6.79 (d, 1H, $J = 7$ Hz, Ar), 7.04–7.05 (d, 1H, $J = 10$ Hz, Ar), 7.24 (s, 1H, Ar), 7.31–7.34 (q, 1H, $J = 10$ Hz, $J = 9$ Hz, Ar), 7.41–7.44 (d, 1H, $J = 14$ Hz, Ar), 7.74–7.76 (d, 1H, $J = 8$ Hz, Ar), 8.42–8.43 (d, 1H, $J = 3.5$ Hz, Ar), 8.55 (s, 1H, Ar), 8.844 (s, 1H, NH), 10.24 (s, 1H, OH). ^{13}C-NMR (125 MHz, DMSO-*d_6, ppm*) δ: 56.02, 56.79, 112.20, 116.08, 118.07, 119.27, 120.52, 121.51, 124.44, 128.54, 129.93, 135.80, 138.78, 144.24, 145.39, 151.35, 167.12. Anal. Calcd. (%) for $C_{17}H_{17}NO_4$ (299.32): C, 68.22, H, 5.72, N, 4.68; Found: C, 67.41, H, 5.63, N, 4.11.

(E)-3-(4-hydroxy-3-methoxyphenyl)-N-(4-methoxyphenyl)acrylamide ***(VIIg)***

Yield: 83 %. Crystalline, buff-yellow. mp: 136–138 °C. FT-IR (KBr, cm^{-1}): 3436, 3359, 1686, 1661, 1620, 1526, 1471, 1429, 1381, 1334, 1271, 1215, 1147, 1034. ^{1}H-NMR (500 MHz, DMSO-*d_6, ppm*) δ: 3.71 (s, 3H, OCH_3), 3.80 (s, 3H, OCH_3), 6.34–6.37 (d, 1H, $J = 15$ Hz, Ar), 6.77–6.79 (d, 1H, $J = 8$ Hz, Ar), 7.05–7.07 (d, 1H, $J = 8$ Hz, Ar), 7.25 (s, 1H, Ar), 7.36–7.37 (d, 2H, $J = 5$ Hz, Ar), 7.42–7.45 (d, 1H, $J = 15$ Hz, Ar), 8.47–8.48 (d, 2H, $J = 5$ Hz, Ar), 8.89 (s, 1H, NH), 10.23 (s, 1H, OH). ^{13}C-

NMR (125 MHz, DMSO-d_6, *ppm*) δ: 56.08, 56.58, 112.45, 116.02, 118.26, 120.81, 121.40, 127.74, 129.52, 132.80, 134.87, 144.45, 145.49, 151.67, 167.38. Anal. Calcd. (%) for $C_{17}H_{17}NO_4$ (299.32): C, 68.22, H, 5.72, N, 4.68; Found: C, 67.07, H, 5.61, N, 3.99.

*Synthesis of N,N'-ethylen-Bis[(E)-3-(4-hydroxy-3-methoxyphenyl)-acrylamide] (**IXa**)*

Yield: 93 %. Crystalline, yellowish-brown. mp: 146–148 °C. FT-IR (cm-1): 3431, 3146, 2904, 1641, 1599, 1556. 1H-NMR (500 MHz, DMSO-d_6, *ppm*) δ: 3.47–3.50 (t, 4H, J = 15 Hz, J = 7.5 Hz, 2 × CH2), 3.79 (s, 6H, 2 × OCH3), 5.48 (s, 2H, 2 × NH), 6.28–6.31 (d, 2H, J = 15 Hz, Ar), 6.75–6.77 (d, 2H, J = 10 Hz, Ar), 6.95–6.97 (d, 2H, J = 8 Hz, Ar), 7.19 (s, 2H, Ar), 7.25–7.28 (d, 2H, J = 13 Hz, Ar), 10.22 (s, 2H, 2 × OH). 13C-NMR (125 MHz, DMSO-d_6, *ppm*) δ: 39.002, 56.320, 112.070, 116.302, 118.444, 120.585, 128.445, 143.135, 144.412, 151.447, 166.298. Anal. Calcd. (%) for $C_{22}H_{24}N_2O_6$ (412.44): C, 64.07; H, 5.87; N, 6.79; Found: C, 63.48; H, 5.79; N, 6.37.

*N,N'-(trimethylene)-Bis[(E)-3-(4-hydroxy-3-methoxyphenyl)-acrylamide] (**IXb**)*

Yield: 97 %. Crystalline, antique-white. mp: 114–116 °C. FT-IR (cm^{-1}): 3534, 3436, 3013, 2916, 1639, 1592, 1566, 1551. ^{1}H-NMR (500 MHz, DMSO-d_6, *ppm*) δ: 1.95–1.98 (m, 2H, CH_2), 2.92–2.95 (m, 4H, 2 × CH_2), 3.78 (s, 6H, 2 × OCH_3), 5.48 (s, 2H, 2 × NH), 6.29–6.32 (d, 2H, J = 15 Hz, Ar), 6.75–6.77 (d, 2H, J = 10 Hz, Ar), 6.96–6.98 (d, 2H, J = 9 Hz, Ar), 7.19 (s, 2H, Ar), 7.25–7.28 (d, 2H, J = 13 Hz, Ar), 10.22 (s, 2H, 2 × OH). ^{13}C-NMR (125 MHz, DMSO-d_6, *ppm*) δ: 28.41, 39.01, 56.74, 112.07, 116.31, 118.42, 120.66, 128.04, 143.11, 144.90, 151.46, 166.89. Anal. Calcd. (%) for $C_{23}H_{26}N_2O_6$ (426.46): C, 64.78; H, 6.15; N, 6.57; Found: C, 64.01; H, 6.08; N, 6.29.

*N,N'-propylen-Bis[(E)-3-(4-hydroxy-3-methoxyphenyl)-acrylamide] (**IXc**)*

Yield: 93 %. Crystalline, apricot color. mp: 94–96 °C. FT-IR (cm^{-1}): 3436, 3197, 2935, 1596, 1591, 1582, 1566. ^{1}H-NMR (500 MHz, DMSO-d_6, *ppm*) δ: 1.40–1.43 (d, 3H, J = 14 Hz, CH_3), 2.76–2.78 (q, 1H, J = 7 Hz, J = 4 Hz, CH), 3.70 (s, 3H, OCH_3), 3.79 (s, 3H, OCH_3), 4.77–4.80 (d, 2H, J = 15 Hz, CH_2), 6.33–6.37 (d, 1H, J = 19 Hz, Ar), 6.77–6.79 (d, 1H, J = 8 Hz, Ar), 7.01–7.03 (d, 1H, J = 10.5 Hz, Ar), 7.21 (s, 1H, Ar), 7.24–7.27 (t, 1H, J = 12.5 Hz, J = 7 Hz, Ar), 7.35–7.38 (d, 1H, J = 16 Hz, Ar), 7.44–7.46 (d, 1H, J = 8 Hz, Ar), 7.56–7.88 (t, 2H, J = 13 Hz, J = 7.5 Hz, Ar), 8.49–8.51 (d, 1H, J = 5 Hz, Ar), 8.98 (s, 2H, 2 × NH), 10.31 (s, 2H, 2 × OH). ^{13}C-NMR (125 MHz, DMSO-d_6, *ppm*) δ: 17.99, 46.09, 47.95, 56.31, 112.09, 116.83, 118.58, 120.69, 127.89, 143.11, 144.23, 151.25, 166.44. Anal. Calcd. (%) for $C_{23}H_{26}N_2O_6$ (426.46): C, 64.78; H, 6.15; N, 6.57; Found: C, 64.14; H, 6.11; N, 6.01.

*N,N'-butylen-Bis[(E)-3-(4-hydroxy-3-methoxyphenyl)-acrylamide] (**IXd**)*

Yield: 95 %. Crystalline, brown. mp: 136–138 °C. FT-IR (cm^{-1}): 3401, 3188, 2935, 1642, 1617, 1589, 1561. ^{1}H-NMR (500 MHz, DMSO-d_6, *ppm*) δ: 1.94–1.97 (t, 4H, J = 15 Hz, J = 12.5 Hz, 2 × CH_2), 2.93–2.96 (t, 4H, J = 15 Hz, J = 7.5 Hz, 2 × CH2), 3.75 (s, 6H, 2 × OCH_3), 5.43 (s, 2H, 2 × NH), 6.29–6.32 (d, 2H, J = 15 Hz, Ar), 6.75–6.78 (d, 2H, J = 10 Hz, Ar), 6.95–6.97 (d, 2H, J = 9 Hz, Ar), 7.19 (s, 2H, Ar), 7.25–7.27 (d, 2H, J = 13 Hz, Ar), 10.27 (s, 2H, 2 × OH). ^{13}C-NMR (125 MHz, DMSO-d_6, *ppm*) δ: 27.42, 41.95, 56.34, 112.09, 116.33, 118.21, 120.18, 127.99, 143.51, 144.43, 151.46, 166.17. Anal. Calcd. (%) for $C_{24}H_{28}N_2O_6$ (440.49): C, 65.44; H, 6.41; N, 6.36; Found: C, 64.89; H, 6.33; N, 5.97.

*N,N'-3-(4-(3-aminopropyl)piperazin-1-yl)propylen)-Bis[(E)-3-(4-hydroxy-3-methoxyphenyl)-acrylamide] (**IXe**)*

Yield: 89 %. Crystalline, brown. mp: 130–132 °C. FT-IR (cm^{-1}): 3371, 3163, 1647, 1612, 1589, 1572. ^{1}H-NMR (500 MHz, DMSO-d_6, *ppm*) δ: 1.89–1.92 (t, 4H, J = 15 Hz, J = 7.5 Hz, 2 × CH_2), 2.82–2.85 (t, 12H, J = 15 Hz, J = 7.5 Hz, 6 × CH_2), 3.88 (s, 6H, 2 × OCH_3), 3.95–3.98 (m, 4H, 2 × CH_2), 5.42 (s, 2H, 2 × NH), 6.31–6.34 (d, 2H, J = 15 Hz, Ar), 6.75–6.77 (d, 2H, J = 10 Hz, Ar), 6.97–6.99 (d, 2H, J = 9 Hz, Ar), 7.11 (s, 2H, Ar), 7.24–7.27 (d, 2H, J = 15 Hz, Ar), 10.24 (s, 2H, 2 × OH). ^{13}C-NMR (125 MHz, DMSO-d_6, *ppm*) δ: 27.11, 38.01, 51.51, 53.52, 56.45, 112.33, 116.83, 118.21, 120.23, 127.86, 143.13, 144.83, 151.11, 166.12. Anal. Calcd. (%) for $C_{30}H_{40}N_4O_6$ (552.66): C, 65.20; H, 7.30; N, 10.14; Found: C, 64.89; H, 7.21; N, 9.93.

Cytotoxicity assay

A variety of human cancer cell lines (breast: MCF-7 and MDA-MB-231, lung: A549, Cervical: HeLa and liver: HepG2) and one normal stem cell line (BM-MSC) were acquired from National Centre for Cell Sciences, Pune, India, for primary screening of synthesized molecules as

strong anticancer agents. The cells were grown in the tissue culture flasks at 37 °C within the carbon dioxide incubator (5 % CO_2, 90 % RH) by using growth medium which contained the RPMI-1640 medium (with 2 mM glutamine), supplemented with 10 % fetal bovine serum, 100 µg/mL streptomycin and 100 units/mL penicillin at pH 7.4. In brief, 5×10^3 cells in 200 ml of medium were seeded in 96-well Elisa plates. Serial dilutions of tested synthesized derivatives ranging from 0 to 100 mM in DMSO have been putted to the monolayer, and 0.1 % DMSO was used as vehicle control during MTT assay. After 24 h of cell culture, 50 ml (5 mg/ml) of MTT was added in the culture plates and incubated at 37 °C for 4 h in CO_2 incubator under dark. MTT mixed culture plates were aspirated; 25 ml of Sorensen glycine buffer (0.1 M glycine and 0.1 M NaCl, pH 10.5) with 200 ml of DMSO have been added into the plates to lyse the cells and for the solubilization of the water insoluble formazones (Sondhi *et al.,* 2012; Kumar *et al.,* 2014). Finally, the absorbance of all the lysates were taken at 570 nm with the help of Fluostar optima microplate reader (BMG Labtech, Germany). The IC_{50} values were calculated by using the software GraphPad Prism 5.02, and the percentage inhibition was calculated with the help of mathematical formula which is given below:

$$\frac{\text{Mean OD of vehicle treated cells (negative control)} - \text{Mean OD of treated cells}}{\text{Mean OD of vehicle treated cells (negative control)}} \times 100$$

DPPH assay

The earlier reported methods for antioxidant assays with modifications were used here to determine the spectral values of ferulic acid amide derivatives (Blois, 1958; Sharma and Bhat, 2009; Vashisth *et al.,* 2015). The currently used method of microplate assay has its own benefits. It is environmental friendly and also reduces the time and sample as compared to the commonly used in vitro antioxidant methods (labor, time, sample and reagent consuming) for testing of antioxidant activity of the compounds. Briefly, the methanolic DPPH solution (50, 100 µg/mL) was added into each sample of different concentration (200 µL, 12.5–100 µg/mL). The solutions (sample with DPPH) were mixed gently and incubated for 30 min in the dark at room temperature, and absorbance was recorded at 517 nm. Different concentrations of methanolic DPPH (5–50 µg/mL) have been taken in the formation of standard curve. The concentration of DPPH in the reaction mixture was calculated according to the method reported earlier (Li *et al.,* 2012a, b). The scavenging capability of test compounds was calculated using the following equation:

$$\text{Percentage DPPH radical scavenging activity} = \left(1 - \frac{\lambda 517 - S}{\lambda 517 - C}\right) \times 100$$

where $\lambda_{517\text{-C}}$ is absorbance of a control with no radical scavenger and $\lambda_{517\text{-S}}$ is absorbance of the remaining DPPH in the presence of scavenger.

3D-QSAR modeling

Five CoMFA models based on the anticancer activities of 21 compounds and one CoMFA model based on the antioxidant activity of 34 compounds have been generated. The pIC_{50} values exhibited by the synthesized derivatives were used as the dependent variable for the generation of CoMFA model. SYBYL7.1 (Silicon Graphics Octane2 workstation containing IRIX6.5 operating system) was used for all the calculations performed during the molecular modeling exercise. The PM3 method was applied for the energy minimization step with 0.005 kcal/mol energy gradient convergence criterion, and the Gasteiger-Huckel charges were assigned to all the compounds during their modeling (Gasteiger and Marsili, 1980). The random selections have been made to choose the training and test set compounds for anticancer (16 and 5 compounds) and antioxidant model (26 and 8 compounds). The database alignment method was applied for the alignment of molecules and selected the lowest energy conformer of the most active compound as a template (Fig. S35). The Comparative Molecular Field Analysis (CoMFA) method was executed for the evaluation of steric and electrostatic fields and partial least square (PLS) analysis was also carried out to correlate the CoMFA fields with experimentally exhibited biological activities by amide derivatives (Cramer *et al.,* 1988a, b; Wold, 1991). The leave-one-out (LOO) method has been used for the cross-validation (r^2_{cv}) of data, and the formula given below was used for the calculation of predictive correlation (r^2_{pred}):

$$r^2_{pred} = (SD - PRESS)/SD$$

where SD is the sum of the squared deviations between the test set biological activities and mean activities of the

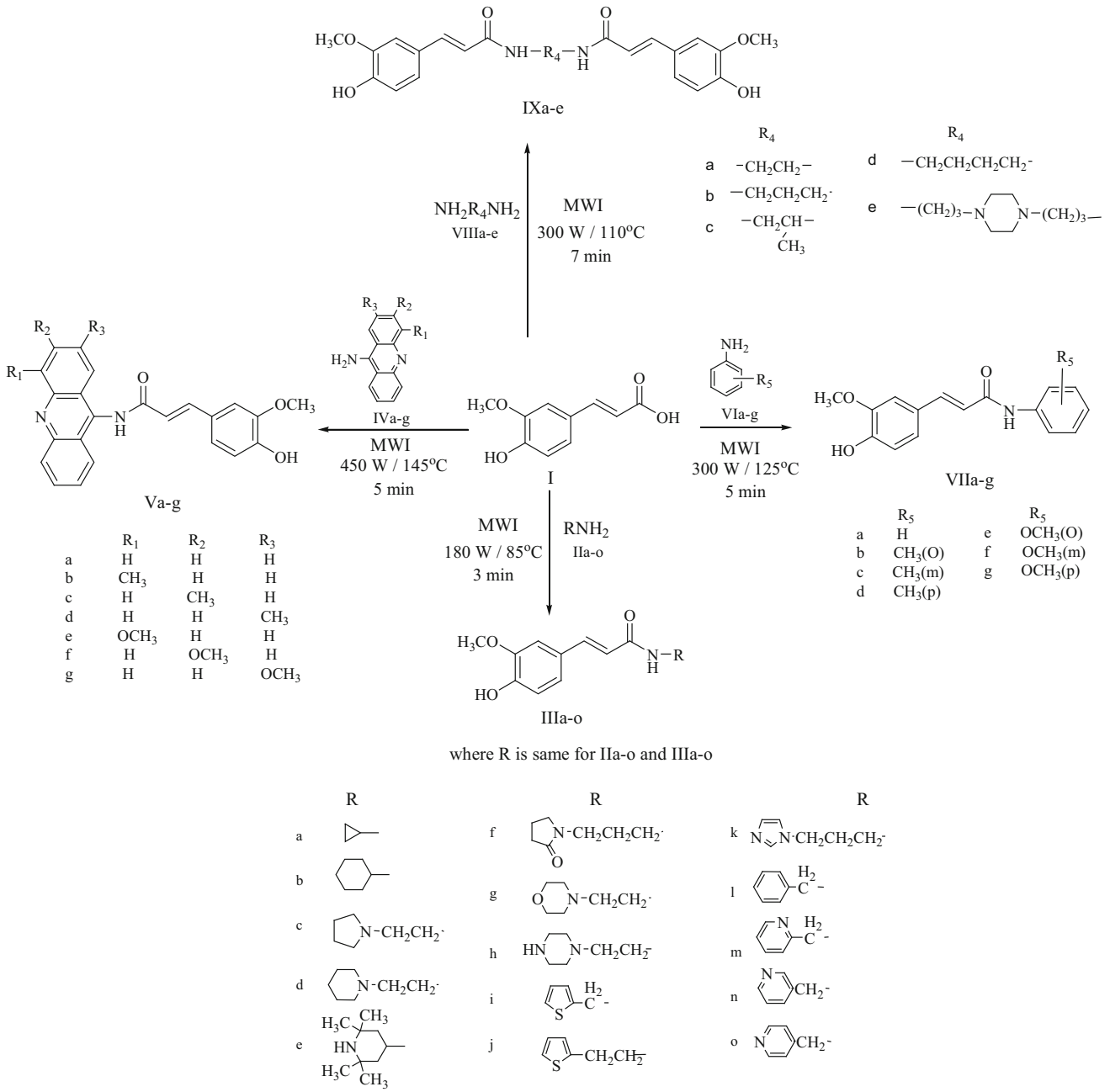

Scheme 1 Schematic representation of synthesis of amide derivatives of ferulic acid, i.e., **IIIa–IIIo, Va–Vg, VIIa–VIIg** and **IXa–IXe**

training set molecules and PRESS is the sum of the squared deviations between the actual and predicted activities of the test compounds (Cramer *et al.,* 1988a, b).

Statistical analysis

The values of pIC_{50} for anticancer and antioxidant activities of all the derivatives obtained experimentally and theoretically have been tested statistically for their mathematical validation by using MATLAB R2013a toolbox. The correlation coefficient (R) value, which measures the potency and direction of a linear association between two variables, was calculated between simulated and experimental data (Kumar and Bhalla, 2011; Kumar and Garg, 2014; Goel and Singh, 2013; Goel and Kumar, 2014). All the experiments were carried out in triplicate for reproducing the results, and the mean values were taken for the comparison of data.

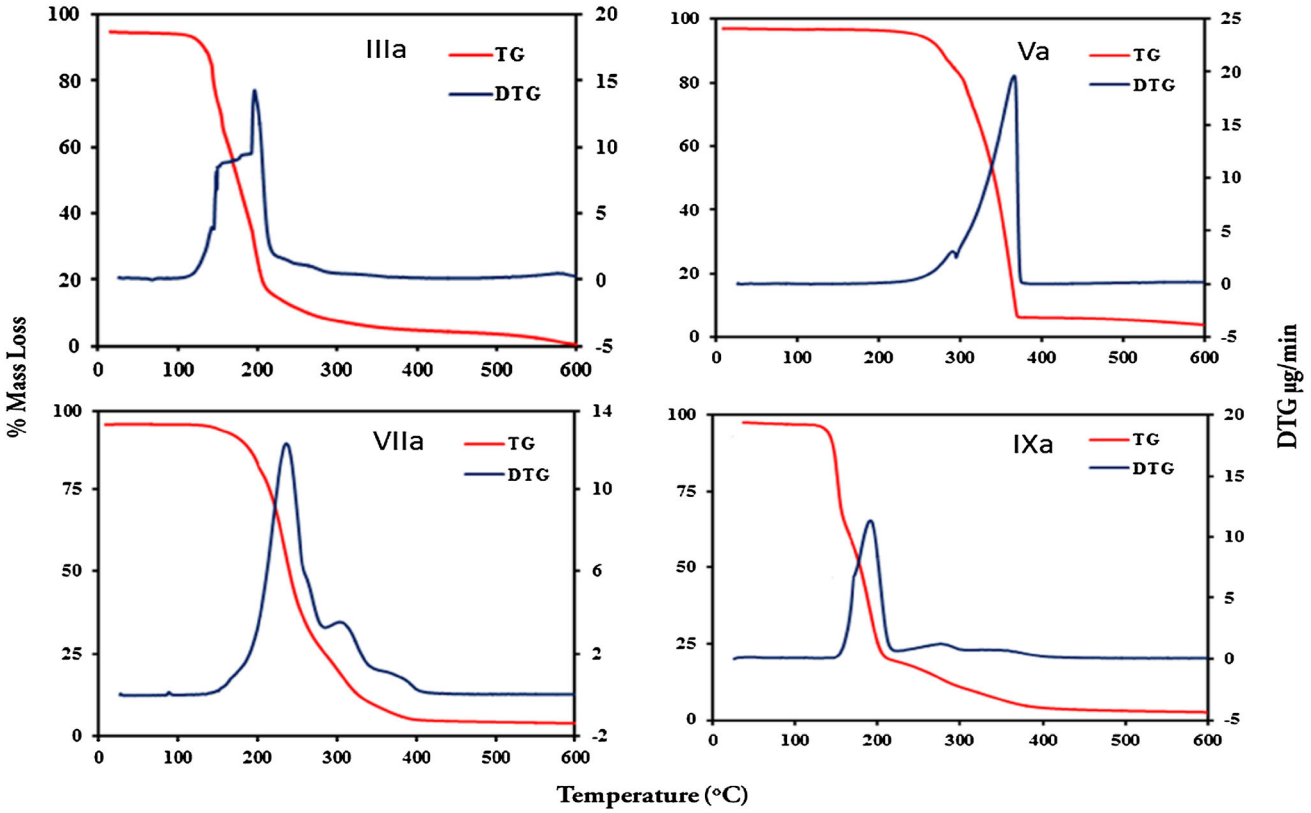

Fig. 1 Simultaneous TG-DTG thermogram of **IIIa, Va, VIIa** and **IXa** under nitrogen

Results and discussions

Chemistry

Microwave-assisted synthesis of four series of mono and bis-amide derivatives of ferulic acid has been achieved at room temperature by simple grinding of the mixture of ferulic acid and corresponding amines (**IIa–IIo**, **IVa–IVg**, **VIa–VIg** and **VIIIa–VIIIe**; Scheme 1) in 1:1 and 1:2 molar ratio within 3–7 min. All the molecules were well characterized by highly sophisticated techniques including FT-IR, FT-NMR, mass spectroscopy, TGA-DTG thermal analysis as well as elemental analysis for C, H and N. The structural data obtained from spectral (Fig. S1–Fig. S34) and elemental studies for the compounds reported in the experimental section have fully supported the chemical structures assigned to them. The ^{1}H-NMR spectra for all the compounds did not show any change after keeping them for 10 days at room temperature; similarly the same spectra were also collected after 6 months when compared with the previous data and found negligible changes in the results with respect to the starting spectroscopic data. Commencing on the results from above studies, we can conclude that the currently synthesized amide derivatives are stable in solid as well liquid phase even after a long interval of time.

Thermal analysis

Thermal behavior of a molecule is exciting predicting their stability, shelf lives and suitable storage conditions (Shamsipur *et al.,* 2013). Thermokinetic data could be calculated by thermal analysis, which makes the possible determination of thermodynamic parameters for a drug candidate (Lever and Papadaki, 2004). Here, all the derivatives, like their parent molecule (ferulic acid), were found stable up to 100 °C and decomposed through one step during thermal studies. After 100 °C, the TG-DTG curves showed irregular pattern which confirmed the maximum decomposition. The graphical representation of thermal analysis curves for the first compound from each series is shown in Fig. 1, and the details of results are provided in Table S1. The compound **IIIa** was decomposed immediately after melting, and it continued up to 364 °C with 98.1 % weight loss (DTG peak at 205 °C), which corresponds to endotherm at 292 °C in DTA. In **Va**, the weight loss (97.6 %) was observed in the temperature range of 264–378 °C (DTG peak at 341 °C). The thermal decomposition of **VIIa** occurred in the temperature range of 174–402 °C, which showed the weight loss of 97.9 % with the DTG peak at 257 °C, while **IXa** decomposed in the 148–367 °C temperature range with

Table 1 In vitro anti-proliferative activity (% growth inhibition) of ferulic acid amide derivatives (10 μM concentration)

Compound name	Breast (MCF-7)	Breast (MDA-MB-231)	Lung (A549)	Liver (HepG2)	Cervical (HeLa)	Normal (stem)
IIIa	29.19	16.98	26.17	27.69	22.73	NA
IIIb	27.95	30.18	19.07	34.94	31.88	NA
IIIc	23.51	21.77	27.28	20.65	25.68	NA
IIId	32.30	24.22	33.89	25.14	29.22	NA
IIIe	27.72	21.87	35.52	29.69	32.17	NA
IIIf	26.85	27.22	31.13	29.92	30.24	NA
IIIg	20.28	29.29	17.81	24.93	23.74	06.63
IIIh	25.35	30.55	31.12	29.75	27.93	NA
IIIi	59.09	51.48	54.04	53.55	65.62	11.36
IIIj	62.55	56.83	56.81	50.63	61.91	13.63
IIIk	43.36	47.77	52.27	51.39	55.71	07.68
IIIl	51.92	56.55	56.12	47.68	58.42	18.37
IIIm	58.22	55.09	58.34	44.72	55.43	14.21
IIIn	55.88	57.68	53.42	51.09	53.14	15.34
IIIo	50.81	58.33	56.49	41.62	54.11	08.44
Va	57.24	60.82	69.95	59.36	78.11	17.24
Vb	75.53	77.25	72.64	61.95	71.39	16.47
Vc	66.64	74.10	75.10	63.35	69.19	12.49
Vd	68.97	78.11	79.17	66.46	82.95	06.63
Ve	66.26	62.84	78.56	63.51	81.01	09.76
Vf	79.11	61.12	80.63	66.37	70.97	17.05
Vg	78.04	69.51	83.71	68.32	73.82	19.13
VIIa	51.67	51.91	60.26	45.35	63.41	08.44
VIIb	48.62	43.88	61.03	48.35	59.42	12.69
VIIc	49.68	47.82	53.34	52.33	55.84	08.96
VIId	51.63	55.14	65.88	55.91	60.69	10.27
VIIe	39.07	40.78	58.42	46.58	54.48	08.01
VIIf	42.68	49.83	55.49	50.46	57.28	06.25
VIIg	48.63	55.66	60.65	56.68	63.98	03.68
IXa	24.01	19.09	27.18	25.77	29.09	NA
IXb	33.63	25.02	31.76	20.96	32.95	NA
IXc	27.57	22.24	31.64	23.76	38.01	NA
IXd	28.96	19.95	27.51	22.67	23.59	05.59
IXe	26.91	19.37	27.19	22.59	16.92	08.61
Ferulic acid	23.56	20.18	20.66	21.09	21.91	NA
5 Fluorouracil	15.54	20.22	30.17	32.72	23.84	25.21
Cyclophosphamide	13.17	15.84	11.18	19.50	20.16	19.27
Cycloheximide	15.22	17.96	14.11	22.13	22.37	23.98

NA not applicable

mass loss of 98.9 % (DTG peak at 198 °C). Other compounds of all the series also exhibited the same stability behavior.

In vitro cytotoxicity

The evaluation of in vitro cytotoxicity of synthesized derivatives (**IIIa–IIIo, Va–Vg, VIIa–VIIg** and **IXa–IXe**) have been calculated by MTT assay as primary screening against the five different human cancer cell lines, i.e., breast (MDA-MB-231 and MCF-7), cervical (HeLa), lung (A549) and liver (HepG2) along with one normal (non-cancerous) cell line at a concentration of 10 μM. The results obtained from these screenings are summarized in Table 1, which confirmed that twenty-one compounds (**IIIi–IIIo, Va–Vg,** and **VIIa–VIIg**) exhibited the noticeable anti-proliferative activity against all tested cancer cell lines and they also showed very less or negligible effect on

Table 2 IC_{50} (μM) values of in vitro anti-proliferative activity of active ferulic acid derivatives

Compound name	Breast (MCF-7)	Breast (MDA-MB-231)	Lung (A549)	Liver (HepG2)	Cervical (HeLa)
IIIi	12.88 ± 3.96	14.08 ± 2.59	13.45 ± 3.35	15.91 ± 3.98	10.97 ± 3.79
IIIj	09.87 ± 2.97	12.97 ± 3.41	13.44 ± 4.02	16.14 ± 3.88	12.07 ± 4.01
IIIk	17.29 ± 1.96	16.91 ± 2.76	12.09 ± 3.72	14.61 ± 3.19	12.26 ± 3.81
IIIl	11.98 ± 3.12	12.28 ± 3.88	12.18 ± 4.12	15.17 ± 3.21	12.05 ± 4.04
IIIm	11.42 ± 3.77	13.06 ± 4.22	12.22 ± 5.03	16.82 ± 4.05	13.71 ± 3.51
IIIn	13.09 ± 4.38	14.32 ± 3.72	12.55 ± 3.09	15.49 ± 3.13	12.83 ± 2.92
IIIo	13.44 ± 2.76	14.91 ± 3.23	13.77 ± 3.54	18.28 ± 3.34	15.82 ± 4.43
Va	09.17 ± 3.47	08.99 ± 3.52	07.84 ± 2.89	10.59 ± 4.27	07.51 ± 3.84
Vb	07.49 ± 3.22	07.29 ± 2.72	08.13 ± 3.11	09.88 ± 4.67	08.75 ± 3.72
Vc	09.23 ± 3.69	07.66 ± 3.36	07.21 ± 3.53	10.21 ± 4.37	08.06 ± 4.19
Vd	08.38 ± 3.64	07.48 ± 3.01	07.11 ± 3.48	09.31 ± 4.05	07.29 ± 3.55
Ve	09.74 ± 3.09	09.89 ± 3.71	07.48 ± 4.52	10.41 ± 3.86	07.14 ± 2.68
Vf	08.06 ± 3.09	10.34 ± 3.19	08.11 ± 3.72	11.08 ± 4.12	08.98 ± 3.18
Vg	08.12 ± 3.88	08.99 ± 3.13	08.04 ± 3.92	10.37 ± 3.79	09.65 ± 4.27
VIIa	13.05 ± 3.72	12.67 ± 3.72	09.77 ± 3.72	15.92 ± 4.29	09.89 ± 3.72
VIIb	15.81 ± 3.65	17.64 ± 3.81	09.19 ± 3.53	13.54 ± 4.78	10.89 ± 3.72
VIIc	15.28 ± 3.37	16.01 ± 3.22	09.16 ± 3.21	12.13 ± 4.09	09.74 ± 3.98
VIId	12.78 ± 3.88	12.49 ± 2.82	08.98 ± 3.56	11.05 ± 3.82	09.53 ± 3.09
VIIe	15.27 ± 3.33	17.04 ± 2.98	11.67 ± 4.01	14.36 ± 2.98	10.62 ± 3.76
VIIf	16.55 ± 3.19	13.14 ± 3.64	10.84 ± 3.09	13.02 ± 3.44	09.87 ± 2.97
VIIg	16.17 ± 3.22	12.74 ± 3.86	09.54 ± 2.64	13.11 ± 3.73	09.17 ± 4.12

the normal stem cells while compounds **IIIa–IIIh** and **IXa–IXe** were found to exhibit very low level of activity. In comparison with their parent molecule, these amide derivatives showed an increased level of anticancer activity. Further, these twenty-one compounds were studied for the calculation of their half maximal inhibitory concentration (IC_{50}) values by serial dilution method, and the results are given in Table 2. On seeing this table, we can conclude that the range of IC_{50} values was laid between 07.11 to 18.28 μM in different kinds of studied cancer cell lines. The amide derivatives which contain the moieties of aliphatic and aromatic amines showed significant anti-proliferative activity and a very low range of inhibitory concentration but the compounds **Va–Vg** (containing acridine moiety) showed the best activity as minimum value of IC_{50} (07.11–11.08 μM) against all the studied cell lines. The most promising compound against breast, lungs, liver and cervical cancer cell lines was **Vb** (IC_{50} values = 7.49 ± 3.22 and 7.29 ± 2.72 μM), **Vd** (IC_{50} values = 7.11 ± 3.48 & 8.31 ± 4.05 μM) and **Ve** (IC_{50} values = 7.14 ± 2.68 μM), respectively.

In vitro antioxidant activity

1,1-Diphenyl-2-Picrylhydrazyl radical (DPPH) is a well-known chemical for the evaluation of free radical scavenging activity of a molecule. It possesses an unpaired electron and produces a stable violet color in methanol solution at 517 nm. The DPPH free radical is reduced into DPPH-H in the presence of hydrogen donating molecule. All the synthesized derivatives have been tested for their antioxidant activity by DPPH assay, and their inhibition constant (EC_{50}) were calculated. The results of in vitro free radical scavenging activities assay given in Table 3 revealed that nine compounds (**IIIf, IIIl, IIIo, VIIe** and **IXa–IXe**) showed superior activity with EC_{50} ranges from 18.37 to 25.44 μM, as compared to the standard ascorbic acid (EC_{50} = 20.14 μM) and isolated ferulic acid (EC_{50} = 34.16 μM). Thirteen derivatives were found to possess poor antioxidant activity having their EC_{50} values ≥35 μM, while twelve compounds exhibited moderate activity with the EC_{50} value between 26.89 and 34.81 μM. The experiments were repeated for three times for reproducing the obtained results and their statistical analyses. Among all synthesized derivatives, **IXa** was found to be the most active molecule during the DPPH assay with EC_{50} value of 18.37 ± 2.74 μM. From the above results, it is clear that the amide derivatives, like their parent molecule, also showed the antioxidant activity. This is due to the presence of phenoxy radical and resonance stabilization which are also present in the ferulic acid. Compounds from bis-amide series (**IXa–IXe**) have two phenolic OH in their

Table 3 EC_{50} (μg/ml) values of free radical scavenging activity of active ferulic acid derivatives

Compound	EC_{50}
IIIa	46.83 ± 3.48
IIIb	31.54 ± 2.74
IIIc	38.85 ± 3.49
IIId	36.28 ± 2.94
IIIe	47.29 ± 3.27
IIIf	23.39 ± 3.84
IIIg	28.11 ± 2.72
IIIh	34.28 ± 2.46
IIIi	28.65 ± 2.79
IIIj	26.94 ± 3.26
IIIk	42.83 ± 3.62
IIIl	19.87 ± 3.32
IIIm	29.78 ± 3.71
IIIn	28.19 ± 3.63
IIIo	25.44 ± 3.67
Va	36.55 ± 3.62
Vb	45.58 ± 4.28
Vc	48.41 ± 3.54
Vd	49.95 ± 4.34
Ve	35.24 ± 3.72
Vf	41.17 ± 3.82
Vg	37.96 ± 3.68
VIIa	27.14 ± 3.57
VIIb	37.73 ± 2.97
VIIc	33.12 ± 2.83
VIId	34.81 ± 2.79
VIIe	23.64 ± 3.73
VIIf	32.78 ± 2.96
VIIg	27.43 ± 3.37
IXa	18.37 ± 2.74
IXb	20.09 ± 2.77
IXc	21.81 ± 2.56
IXd	20.89 ± 3.52
IXe	24.68 ± 2.69
Ferulic acid	34.16 ± 2.52
Ascorbic acid	16.64 ± 1.51

structures, so they can donate 2 protons with DPPH; thus, these molecules were found better antioxidant agents among all derivatives. These molecules were also found to exhibit improved antioxidant activity as compared to curcumin ($EC_{50} = 29.99 \pm 0.39$), a natural antioxidant also having two phenolic OH (Shang *et al.,* 2010). We have also found a positive correlation between antioxidant and anticancer activity of synthesized amides. Compounds (**IIIf**, **IIIl**, **IIIo**, and **VIIe)** showed a noticeable increase in its biological activities as compared to ferulic acid.

Analysis of 3D-QSAR results

Based on the results of in vitro biological activities, we have developed a total of six (6) CoMFA models to find out the structure activity relationship among the synthesized amide derivatives of ferulic acid. The pictorial representation of each model has been shown in Fig. 2. These models were further studied on the basis of contour maps and mathematical factors such as steric-electrostatic contributions, cross-validation coefficient (r^2_{cv}), non-cross-validation coefficient (r^2_{ncv}), predictive correlation coefficient (r^2_{pred}) and the standard error of estimation (SEE). The data used as input in the generation of CoMFA models are provided as Table S2 and Fig. S36. The final values of studied factors are summarized in Table 4, which was generated after the statistical analysis of data. In the CoMFA models for breast (Fig. 2a, b), lung (Fig. 2c) and liver (Fig. 2d) cancer cells and DPPH assay (Fig. 2f) showed significantly high steric contributions as compared to electrostatic one, while in case of cervical cancer cells (Fig. 2e) the electrostatic contribution is slightly higher than steric interactions indicating their roles in the variation of biological activities of synthesized derivatives. These results are also confirmed by the statistical validation of data (Table 4). In the CoMFA model for MCF-7 cells, green contours were observed close to o-position and yellow contours around rest of the acridine ring indicated that the increasing and decreasing steric bulk at these position, respectively, would results in the enhanced bioactivities. This is an established fact that compounds with higher pIC_{50} values have bulky substituents at o-position of acridine ring and no bulky group was noticed near other positions of acridine ring. The two small red contours near the central and un-substituted acridine rings positions were observed, while blue contour was observed at substituted bulky group of acridine ring. The red contour signifies the presence of electron-rich regions, whereas the blue contour corresponds to the regions where an increased positive charge would result in boost up of bioactivity. In the MDA-MB-231 CoMFA model, green contour was observed near the o-position of acridine ring while a slight disagreement was noticed for the yellow colored contours as compared to MCF-7 cells. The number of bulky disfavored regions is less for the MDA-MB-231 model. More importantly in MCF-7 model, the m- and p-positions of the substituted acridine ring are demonstrated with yellow contour indicating it as sterically disfavored while the same site has been demonstrated with green contours in MDA-MB-231 indicating that at these regions the steric bulk is favored for increasing the biological activity. The similar region in the models of A549 and HeLa cells was also demonstrated by green contours (Fig. 2c, e). Unlike the breast cancer models, these models disfavor steric bulk at the o-position

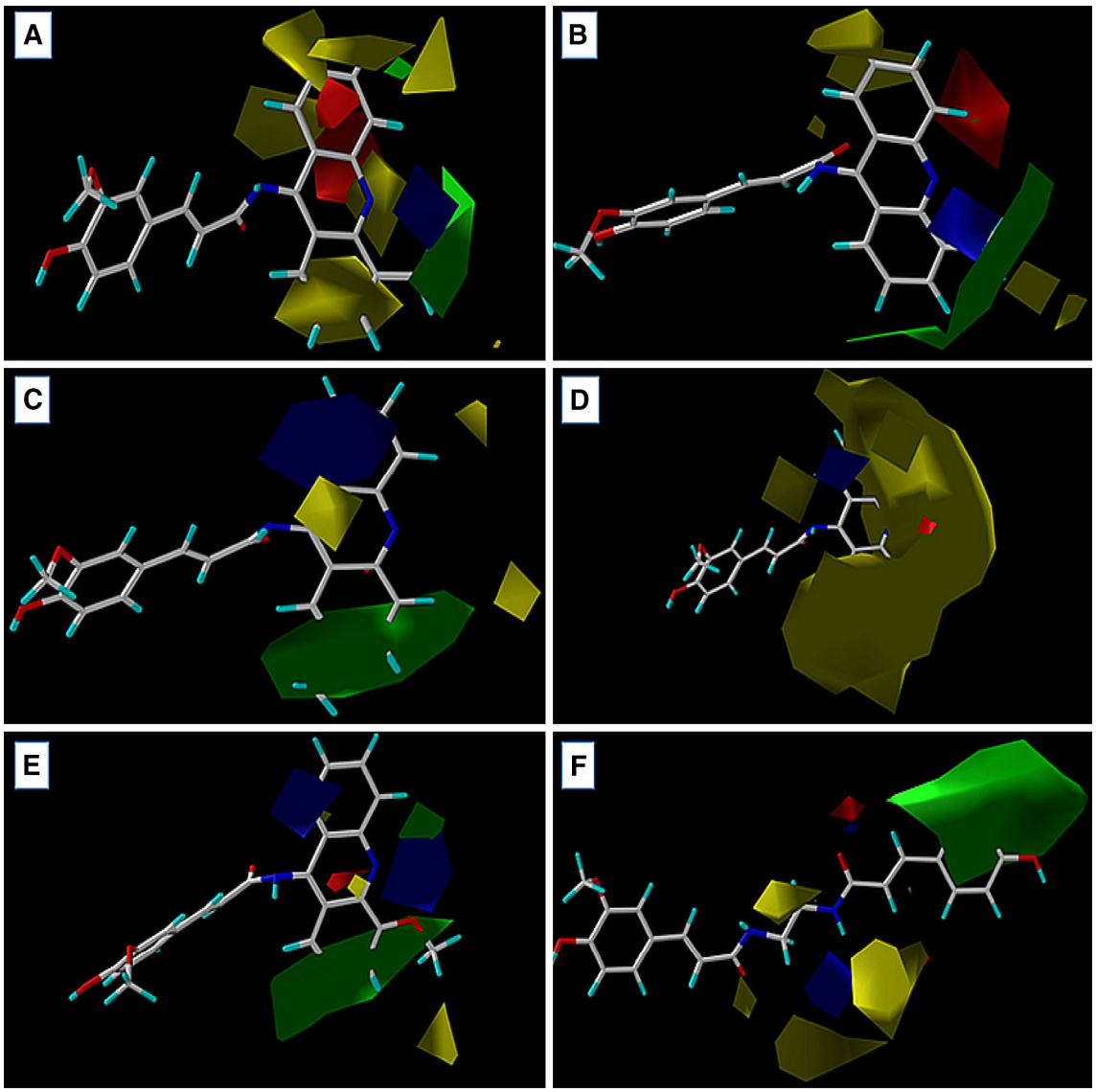

Fig. 2 STDDEV*COEFF plots of the CoMFA steric and electrostatic contour maps for **a** MCF-7 **b** MDA-MB-231 **c** A549 **d** HepG2 **e** HeLa **f** antioxidant models. (The most active molecule is displayed in the background. Green region sterically favored, yellow region sterically disfavored, red region negatively charged favored, and blue region positively charged favored) (Color figure online)

of acridine ring. Moreover, positively charged substituents are favored at the unsubstituted acridine ring (indicated by blue contours) in both the models, the effect being more pronounced in case of A549 cells. Positively charged substituents are also favored near o-position (toward ferulic acid) of unsubstituted acridine ring. In the HepG2 model, steric contribution was found to be relatively higher than electrostatic contribution and the same was also noticed in contour maps (Fig. 2d). In this model, steric bulk is highly disfavored around the acridine ring (as can be seen from the cloud of yellow contour around the acridine ring). Small blue contour was found around the o-position of unsubstituted acridine ring, very similar to A549 and HeLa cells CoMFA models, suggesting the importance of the positively charged group. In the antioxidant model (Fig. 2f), green and yellow contours were observed around terminal ring and linker region, while blue contour around –NH group of linker chain and red contour near carbonyl group suggest the importance of positively and negatively charged substitutions at these positions. On a comparative scale, the negative charge substituents contributes more in the breast cancer cell lines, while in all other cases very small red contours were noticed.

Analysis of statistical results

The statistical analysis has been done by curve fitting analysis to validate the experimental and theoretical data obtained from biological and computational studies,

Table 4 CoMFA analysis for anticancer and antioxidant activities of ferulic acid derivatives (Grid spacing = 2.0 Å)

Parameters	Breast (MCF-7)	Breast (MDA-MB-231)	Lung (A549)	Liver (HepG2)	Cervical (HeLa)	Antioxidant
r^2_{cv}	0.712	0.711	0.858	0.767	0.816	0.583
r^2_{ncv}	0.966	0.949	0.991	0.934	0.859	0.903
SEE	0.025	0.031	0.011	0.25	0.039	0.044
ONC	4	4	4	3	5	4
r^2_{pred}	0.915	0.822	0.999	0.884	0.0814	0.792
F value	78.878	51.329	81.318	56.338	85.620	48.960
Field contributions						
Steric	0.653	0.686	0.524	0.595	0.484	0.592
Electrostatic	0.347	0.314	0.476	0.405	0.516	0.408

r^2_{cv} cross-validation correlation coefficient, r^2_{ncv} non-cross-validation correlation coefficient, *SEE* standard error of estimation, *ONC* optimum number of components, r^2_{pred} predictive correlation coefficient, *F value* F test value

respectively. All the experiments performed during anticancer and antioxidant activity evaluations of synthesized molecules have been repeated three times for the minimization of error and statistical validation of data (Table S3). Summary of statistical analysis showed that the values of correlation coefficient (*R*) for all the studied cases lied between 0.8699–0.9872 and 0.8554–0.9764 in training and test sets, respectively. The plots for curve fitting analysis are given in Fig. S36. Commenting on the statistical results, we inferred that simulated values of pIC_{50} statistically are in line with the experimental results and outcome in all the cases is worthy. The reasonable correlation between the experimental and predicted values of biological activities of the training and test set compounds would be used as a guide in designing of new molecules as anticancer and antioxidant agents based on ferulic acid.

Conclusions

Ferulic acid is an imperative natural lead molecule for designing the compounds of biological interest. In this work, thirty four amide derivatives of ferulic acid have been synthesized under solvent-free conditions by microwave-assisted condensation reaction, and fully characterized by spectroscopic techniques. The stability of these amide derivatives have been confirmed by thermal and spectroscopic results. After the successful structural and thermal characterization, the derivatives have been screened for their different biological applications. Twenty-one derivatives (**IIIi–IIIo, Va–Vg,** and **VIIa–VIIg**) were found to exhibit noticeable in vitro anticancer activity against all studied cancer cell lines, while all the derivatives showed negligible effect on normal cells. They were also tested for in vitro free radical scavenging activity; nine compounds were found to exhibit increased activity as compared to ferulic acid. As it is a proven fact that oxidative stress leads to many dreadful human diseases like cancer, we have designed such kind of molecules which are acting both as antioxidant and anticancer agent. It is envisaged that there is a probable relationship between the observed anticancer and antioxidant activity of the amide derivatives. These compounds may serve as a lead molecule in quest of a vital anticancer drug, which will also minimize the oxidative stress started due to various physiological conditions in cells. To further establish the correlation among experimental results, the QSAR analyses were performed, and six different CoMFA models have been generated and analyzed. The statistical analysis, contour maps analysis, and comparison between steric and electrostatic field contribution were carried out to understand the correlation between their chemical structure and biological activities. The results of contour maps analyses aligned with the statistical validation proves the accuracy of these models and statistically significant correlation in all aforesaid discussed cases. Also these outcomes could be used as a base model in the designing of novel amide derivatives of natural phenolics that will lead to a high-quality drug which acts both as anticancer and antioxidant agent. Therefore, they would lead as a possible pharmaceutical supplement.

Supplementary material

All the additional Figures (Figs. S1–S36) containing ^{1}H-NMR, ^{13}C-NMR, mass spectra, Mass fragmentation pattern, alignment of all molecules during 3D-QSAR, with additional Tables (Tables S1–S3) are available in PDF formats.

Acknowledgments Naresh Kumar gratefully acknowledges CSIR, New Delhi, India, for financial assistance, Indian Institute of Technology Roorkee and NIPER Mohali for instrumentation facility.

Compliance with ethical standards

Conflict of interest Authors declare no conflict of interest.

References

Basoglu S, Yolal M, Demirci S, Demirbas N, Bektas H, Karaoglu SA (2013) Design, synthesis and antimicrobial activities of some azole derivatives. Acta Pol Pharm 70(2):229–236

Blois MS (1958) Antioxidant determinations by the use of a stable free radical. Nature 181:1199–1200

Chung SY, Champagne ET (2011) Ferulic acid enhances IgE binding to peanut allergens in Western blots. Food Chem 124(4):1639–1642

Clifford MN (1990) Chlorogenic acids and other cinnamates–nature, occurrence and dietary burden. J Sci Food Agric 79(3):362–372

Cramer RD, Bunce JD, Patterson DE, Frank IE (1988a) Cross-validation, bootstrapping, and partial least squares compared with multiple regression in conventional QSAR studies. Quant Struct Act Relat 7(1):18–25

Cramer RD, Patterson DE, Bunce JD (1988b) Comparative molecular field analysis (CoMFA). 1. Effect of shape on binding of steroids to carrier proteins. J Am Chem Soc 110(18):5959–5967

Ferhat M, Ghorab H, Laggoune S, Ghannadi A, Sajjadi SE, Touzani R, Kabouche A, Kabouche Z (2014) Composition and antioxidant activity of the essential oil of *Thymus dreatensis* from Algeria. Chem Nat Comp 50(4):747–749

Gasteiger J, Marsili M (1980) Iterative partial equalization of orbital electronegativity-a rapid access to atomic charges. Tetrahed 36(22):3219–3228

Goel N, Kumar N (2014) Study of supramolecular frameworks having aliphatic dicarboxylic acids, N, N′-bis(salicyl)ethylenediamine and N, N′-bis(salicyl)butylenediamine. J Mol Struct 1071:60–70

Goel N, Singh UP (2013) Syntheses, structural, computational and thermal analysis of acid-base complexes of picric acid with N-heterocyclic bases. J Phys Chem A 117(40):10428–10437

Herrmann K (1989) Occurrence and content of hydroxycinnamic and hydroxybenzoic acid compounds in foods. Crit Rev Food Sci Nutr 28(4):315–347

Hosoda A, Ozaki Y, Kashiwada A, Mutoh M, Wakabayashi K, Mizuno K, Nomura E, Taniguchi H (2002) Syntheses of ferulic acid derivatives and their suppressive effects on cyclooxygenase-2 promoter activity. Bioorg Med Chem 10(4):1189–1196

Huang GY, Cui C, Wang ZP, Li YQ, Xiong LX, Wang LZ, Yu SJ, Li ZM, Zhao WG (2013) Synthesis and characteristics of (Hydrogenated) ferulic acid derivatives as potential antiviral agents with insecticidal activity. Chem Cent J 7(33):1–12

Kiran T, Alekhya C, Lokesh B, Latha A, Prasad Y, Mounika T (2015) Synthesis, characterization and biological screening of ferulic acid derivatives. J Can Ther 6:917–931

Kumar N, Bhalla TC (2011) In silico analysis of amino acid sequences in relation to specificity and physiochemical properties of some aliphatic amidases and kynurenine formamidases. J Bioinform Seq Anal 3(6):116–123

Kumar N, Garg A (2014) Structural optimization and docking studies of anatoxin-a: a potent neurotoxin. Afr J Biotechnol 13(30):3092–3100

Kumar N, Pruthi V (2014) Potential applications of ferulic acid from natural sources. Biotechnol Rep 4:86–93

Kumar N, Pruthi V (2015) Structural elucidation and molecular docking of ferulic acid from *Parthenium hysterophorus* possessing COX-2 inhibition activity. 3. Biotech 5(4):541–551

Kumar S, Kumar N, Roy P, Sondhi SM (2014) Efficient synthesis of heterocyclic compounds derived from 2,6-dioxopiperazine derivatives and their evaluation for anti-inflammatory and anticancer activities. Med Chem Res 23(9):3953–3969

Kumar N, Pruthi V, Goel N (2015) Structural, thermal and quantum chemical studies of *p*-coumaric and caffeic acids. J Mol Struct 1085:242–248

Lever SD, Papadaki M (2004) Study of condition-dependent decomposition reactions: part I. The thermal behaviour and decomposition of 2-nitrobenzoyl chloride. J Hazard Mater 115(1–3):91–100

Li W, Li N, Tang Y, Li B, Liu L, Zhang X, Fu H, Duan JA (2012a) Biological activity evaluation and structure–activity relationships analysis of ferulic acid and caffeic acid derivatives for anticancer. Bioorg Med Chem Lett 22(19):6085–6088

Li WJ, Cheng XL, Liu J, Lin RC, Wang GL, Du SS, Liu ZL (2012b) Phenolic Compounds and Antioxidant Activities of *Liriope muscari*. Molecules 17(2):1797–1808

Middleton E Jr, Kandaswami C, Theoharides TC (2000) The effects of plant flavonoids on mammalian cells: implications for inflammation, heart disease, and cancer. Pharmacol Rev 52(4):673–751

Mori H, Kawabata K, Yoshimi N, Tanaka T, Murakami T, Okada T, Murai H (1999) Chemopreventive effects of ferulic acid on oral and rice germ on large bowel carcinogenesis. Anticancer Res 19(5A):3775–3783

Mori T, Koyama N, Guillot-Sestier MV, Tan J, Town T (2013) Ferulic acid Is a nutraceutical β-secretase modulator that improves behavioral impairment and Alzheimer-like pathology in transgenic mice. PLoS One 8:1–15

Narang AS, Desai DS, Lu YRI (eds) (2009) Pharmaceutical perspectives of cancer therapeutics. Springer. doi:10.1007/978-1-4419-0131-6_2

Ou S, Kwok KC (2004) Ferulic acid: pharmaceutical functions, preparation and applications in foods. J Sci Food Agric 84(11):1261–1269

Paiva LB, Goldbeck R, Santos WD, Squina FM (2013) Ferulic acid and derivatives: molecules with potential application in the pharmaceutical field. Braz J Pharm Sci 49(3):395–411

Parkesh R, Childs-Disney JL, Nakamori M, Kumar A, Wang E, Wang T, Hoskins J, Tran T, Housman D, Thornton CA, Disney MD (2012) Design of a bioactive small molecule that targets the myotonic dystrophy type 1 RNA via an RNA motif-ligand database and chemical similarity searching. J Am Chem Soc 134(10):4731–4742

Piazzon A, Vrhovsek U, Masuero D, Mattivi F, Mandoj F, Nardini M (2012) Antioxidant activity of phenolic acids and their metabolites: synthesis and antioxidant properties of the sulphate derivatives of ferulic and caffeic acids and of the acyl glucuronide of ferulic acid. J Agric Food Chem 60(50):12312–12323

Rosazza JPN, Huang Z, Dostal L, Volm T, Rousseau B (1995) Review: biocatalytic transformations of ferulic acid: an abundant aromatic natural product. J Ind Microbiol 15(6):457–471

Sajjadi SE, Naderi GH, Ziaii R, Zolfaghari B (2004) The antioxidant activity of polyphenolic fraction of *Thymus daenensis* Celak. Iran J Pharm Res 3(2):80–81

Shamsipur M, Pourmortazavi SM, Beigi AKM, Heydari R, Khatibi M (2013) Thermal stability and decomposition kinetic studies of acyclovir and zidovudine drug compounds. AAPS Pharm Sci Tech 14(1):287–293

Shang YJ, Jin XL, Shang XL, Tang JJ, Liu GY, Dai F, Qian YP, Fan GJ, Liu Q, Zhou B (2010) Antioxidant capacity of curcumin-directed analogues: structure-activity relationship and influence of microenvironment. Food Chem 119:1435–1442

Sharma OP, Bhat TK (2009) DPPH antioxidant assay revisited. Food Chem 113(4):1202–1205

Sondhi SM, Kumar S, Kumar N, Roy P (2012) Synthesis anti-inflammatory and anticancer activity evaluation of some pyrazole and oxadiazole derivatives. Med Chem Res 21(10):3043–3052

Sultana R (2012) Ferulic acid ethyl ester as a potential therapy in neurodegenerative disorders. Biochim Biophys Acta 1822(5): 748–752

Tamm LK, Abildgaard F, Arora A, Blad H, Bushweller JH (2003) Structure, dynamics and function of the outer membrane protein A (OmpA) and influenza hemagglutinin fusion domain in detergent micelles by solution NMR. FEBS Lett 555(1):139–143

Tan Z, Shahidi F (2011) Chemoenzymatic synthesis of phytosteryl ferulates and evaluation of their antioxidant activity. J Agric Food Chem 59(23):12375–12383

Teresa LS, Filipa SC, Maria PMM, Rita C, Tiago S, Jorge G, Nuno M, Fernanda B, Fernanda R, Elisiário TS, Jon H, Paulo JO (2011) Lipophilic caffeic and ferulic acid derivatives presenting cytotoxicity against human breast cancer cells. Chem Res Toxicol 24(5):763–774

Toshihiro A, Ken Y, Miho Y, Motohiko U, Yumiko K, Naoto S, Koichi A (2000) Triterpene alcohol and sterol ferulates from rice bran and their anti-inflammatory effects. J Agric Food Chem 48(6):2313–2319

Vashisth P, Kumar N, Sharma M, Pruthi V (2015) Biomedical applications of ferulic acid encapsulated electrospun nanofibers. Biotechnol Rep 8:36–44

Wang F, Lu W, Zhang T, Dong J, Gao H, Li P, Wang S, Zhang J (2013) Development of novel ferulic acid derivatives as potent histone deacetylase inhibitors. Bioorg Med Chem 21(22):6973–6980

Wiegand C, Heinze T, Hipler UC (2009) Comparative in vitro study on cytotoxicity, antimicrobial activity, and binding capacity for pathophysiological factors in chronic wounds of alginate and silver-containing alginate. Wound Repair Regen 17(4):511–521

Wold S (1991) Validation of QSAR's. Quant Struct Act Relat 10:191–193